



AFRL-OSR-VA-TR-2014-0336

DESCENDING AND LOCAL NETWORK INTERACTIONS CONTROL ADAPTIVE LOCOMOTION

**Roy Ritzmann
CASE WESTERN RESERVE UNIV CLEVELAND OH**

**12/04/2014
Final Report**

DISTRIBUTION A: Distribution approved for public release.

**Air Force Research Laboratory
AF Office Of Scientific Research (AFOSR)/ RTE
Arlington, Virginia 22203
Air Force Materiel Command**

REPORT DOCUMENTATION PAGE

Form Approved
OMB No. 0704-0188

Public reporting burden for this collection of information is estimated to average 1 hour per response, including the time for reviewing instructions, searching existing data sources, gathering and maintaining the data needed, and completing and reviewing this collection of information. Send comments regarding this burden estimate or any other aspect of this collection of information, including suggestions for reducing this burden to Department of Defense, Washington Headquarters Services, Directorate for Information Operations and Reports (0704-0188), 1215 Jefferson Davis Highway, Suite 1204, Arlington, VA 22202-4302. Respondents should be aware that notwithstanding any other provision of law, no person shall be subject to any penalty for failing to comply with a collection of information if it does not display a currently valid OMB control number. **PLEASE DO NOT RETURN YOUR FORM TO THE ABOVE ADDRESS.**

1. REPORT DATE (DD-MM-YYYY)		2. REPORT TYPE	3. DATES COVERED (From - To)		
4. TITLE AND SUBTITLE			5a. CONTRACT NUMBER		
			5b. GRANT NUMBER		
			5c. PROGRAM ELEMENT NUMBER		
6. AUTHOR(S)			5d. PROJECT NUMBER		
			5e. TASK NUMBER		
			5f. WORK UNIT NUMBER		
7. PERFORMING ORGANIZATION NAME(S) AND ADDRESS(ES)			8. PERFORMING ORGANIZATION REPORT NUMBER		
9. SPONSORING / MONITORING AGENCY NAME(S) AND ADDRESS(ES)			10. SPONSOR/MONITOR'S ACRONYM(S)		
			11. SPONSOR/MONITOR'S REPORT NUMBER(S)		
12. DISTRIBUTION / AVAILABILITY STATEMENT					
13. SUPPLEMENTARY NOTES					
14. ABSTRACT					
15. SUBJECT TERMS					
16. SECURITY CLASSIFICATION OF:			17. LIMITATION OF ABSTRACT	18. NUMBER OF PAGES	19a. NAME OF RESPONSIBLE PERSON
a. REPORT	b. ABSTRACT	c. THIS PAGE			19b. TELEPHONE NUMBER (include area code)

AFOSR Annual Report – FA9550-10-1-0054

Descending and Local Network Interactions Control Adaptive Locomotion

11/24/2014

The primary goal of our project is to document common control schemes that allow animals to move seamlessly through very diverse and complex terrain. A common strategy among most animals relies upon hierarchical interactions between circuitry in the brain and local control systems. In arthropods, local control resides in the thoracic ganglia while in vertebrates similar circuits are found in spinal cords (Orlovsky et al., 1999; Ritzmann and Büschges, 2007). Brain circuits process information from numerous sensory systems on the animal's head to monitor its surroundings on a moment-to-moment basis while the more local control circuitry directly controls movements of appendages through interactions between local reflexes and pattern generators. The head sensors provide a large variety of information which is then processed in specific brain regions to ultimately form descending commands. When these commands reach local control regions, they can transiently re-direct the movements of legs or wings. The connections between these control centers assures that movement is efficient and stable while matching it to ever changing conditions in the animal's surrounding environment as well as internal conditions such as hunger, thirst and the need to seek shelter or mates. It is this ability to alter behavior quickly, but in a precise context dependent fashion, that distinguishes agile animal locomotion from autonomous behavior of just about any man-made autonomous vehicle.

The question posed by our proposal was: **How do descending commands exert their influence on local control systems?** Since the local reflexes act in locomotory patterns, while the activity coming from head sensors are typically unpatterned, the manner in which interactions occur is not always obvious. In our proposal, we suggested that a common control scheme could exist in various animals by which descending commands influence movement, not by micromanaging changes, but rather by altering a few critical reflexes then allowing the resulting changes in movement to generate a cascade of additional reflex effects. For example, to evoke climbing, the brain need only direct the rotation of the joints between the thorax and coxa of the middle legs so that extension of other joints now extends the leg downward and pushes the body upward (Watson et al., 2002b). This postural adjustment means that leg extension now experiences greater resistance as the cockroach rears up against gravity and the consequent increase in cuticular strain is detected by campaniform sensilla on the leg. Increased activity in the campaniform sensilla act through local reflexes to increase motor activity, thereby providing the added force needed to push the insect up and over the object in its path (Watson et al., 2002a). Under this strategy, the higher centers work with local systems to influence re-directed movements through critical but subtle changes rather than dictating radically new actions.

To examine this hypothesis, we proposed to look directly at the linkage that occurs between brain and local circuitry when cockroaches transition between walking and turning. To aid in examination of the walking task, we developed, in our previous AFOSR grant, a hardware model based upon neural circuitry that had been documented in stick insects (Ekeberg et al., 2004; Rutter et al., 2008). A new leg now captures the joint movements of the cockroach middle leg, as documented in a paper that describes our 3D joint kinematics motion analysis tool (Bender et al., 2010b). The new leg is also being made to capture the coordinated joint changes that occur in the transition from straight walking to turning as documented in a thesis that was partially supported on the AFOSR grant (Brown, 2011). While this leg project was successful (Klein et al., 2011), we have now expanded into more detailed and very realistic computer simulation of both the mechanics and neural control network for every joint of every leg of the model insect. This simulation based upon all known and implied thoracic connections was developed to account for the cockroach's forward walking movements as well as the transition to turning that we had previously documented (Szczecinski et al., 2014). Because the proposed leg is controlled by realistic reflex circuits, it allows us to formulate new hypotheses that could be further tested with biological experiments. Indeed, the model includes two pairs of descending neurons, whose activity can generate a family of turning

movements in a simulation agent. Moreover, the neural network has been used successfully to control movements of the hardware leg model. Finally, in order to examine how general these control schemes are, we proposed to perform parallel studies on a flight system, focusing upon proprioceptive influences that act on moth flight.

Overview of Results:

Over the duration of our 4 year AFOSR grant we have succeeded in all of our proposed aims and in many cases went well beyond those goals. We documented actions of all leg joints during turning movements and also examined gait changes in freely moving insects. We made great progress in examining the properties of central complex (CX) neurons in both tethered and freely moving insects. These experiments extended our previous discovery of activity preceding changes in walking speed to turning and climbing movements. Our simulation accounted for turning movements in each joint of each leg and suggested mechanisms for descending commands to alter local reflexes in order to evoke such turns. We directly tested this hypothesis by stimulating in the CX through implanted electrodes that had previously evoked turning movements in the same test subject. These experiments verified that stimulation in this brain region does indeed reverse local reflexes in a manner consistent with changes seen in turning. Finally, we extended our observations of brain interactions in walking insects to actions involving a wing mechanoreceptor in the flight behavior of the hawk moth.

Having achieved all of our proposed goals, we then extended our observations to the praying mantis. This close relative to the cockroach provides distinct advantages for testing our hierarchical control hypothesis. As a predator, the mantis stalks its prey and then strikes accurately at it. The targeting that is involved allows us to predict the insect's movements with greater accuracy than is the case with the cockroach. As such, we can relate brain activity to those movements and examine subtle shifts that occur due to manipulation of CX circuitry. Moreover, the predatory behavior changes as the mantis feeds, leading to fewer stalking movements, ultimately resulting in a new ambush strategy. These state dependent changes can be generated through administration of neuromodulatory substances in the insect's blood. In the last year of our AFOSR funding, we successfully transitioned our recording techniques to the praying mantis and developed some new tools for generating very controlled predation tasks while recording from the brain while taking close-up video of the stalking mantis. Our recordings have already revealed interesting neurons whose increased activity is correlated with changes in the mantis's movements. However, when the mantis identifies a prey individual (cockroach nymph), the neuron switches to now monitor actions of that insect. As the mantis stalks its prey, the activity of this neuron in the mantis's CX is closely correlated with movements of the prey. Indeed, the neuron tracks the prey that the mantis is attending to even while ignoring similar nymphs walking through the mantis's field of vision. We are confident that these techniques will allow us to push our understanding of hierarchical control of physiological state dependent behavior much further. A renewal proposal to pursue these additional goals has been submitted to AFOSR.

The following is a more detailed account of our progress to date.

Global Analysis of Three-dimensional Joint Kinematics

Background: In previous years, we described the changes in middle leg movements associated with turning on an oiled plate tether. This tether allows us to hold the cockroach's body relatively still while normal walking leg movements are initiated. As a result, we could examine the changes in leg movements associated with turning that were evoked by tactile contact with one antenna (Mu and Ritzmann, 2005). During turning, the middle and front legs on the outside of the turn rotate laterally, but continue to extend during stance. At the same time, the legs on the inside of the turn now extended during swing, then set down and pulled medially during stance. The hind legs typically make little change in direction, however, the inside hind leg does sometimes simply stop to provide a pivot for strong turns. On a normal substrate the inside front and middle legs would have pulled the animal laterally executing a turn. Under our experimental conditions, these changes were clearly initiated by descending commands originating from tactile stimulation of antennae.

Those earlier studies used very basic motion analysis techniques that made it difficult to document the 3D joint kinematics of each leg. Because 3D kinematics of the front leg posed technical challenges, those early studies analyzed one leg at a time and focused on the middle leg (Mu and Ritzmann, 2005; Mu and Ritzmann, 2008a; Mu and Ritzmann, 2008b). In our previous AFOSR grant, Dr. John Bender began to develop a motion analysis software tool to remove these barriers to analysis. With that tool we could examine the 3D joint kinematics of turning and walking movements in more detail. The software tool was completed on the current grant and used to document the joint kinematics of all joints in all six legs simultaneously as the cockroach walked on an oil-plate tether (Bender et al., 2010b). This study demonstrated that in straight walking, the pattern of joint movements is specific for the various pairs of legs. For example, swing movements in the middle and hind legs are initiated by activation of the trochanter-femur (TrF) joint. This small joint is often ignored and in stick insects it is actually fused to the femur. However, in cockroaches, where the legs attach under the thorax rather than on the lateral surface, the TrF joint is critical for rotating the leg upward at the onset of swing. In contrast, the front leg initiates swing by rotating the joint between the thorax and the coxa (first leg segment). The thorax-coxa (ThC) joint swings dramatically in the front leg, but hardly moves at all in the middle and hind legs. These observations are consistent with the hierarchical model that we are developing for locomotion. It implies that commands that descend from the brain are interpreted and implemented at each leg's local control center in a manner appropriate for that leg. That is, a command to turn left would be implemented differently by the front and hind leg local circuits.

Over the last year, we extended this analysis to data taken during a transition from walking to turning. In these new trials, turning was evoked by presenting a pattern of moving stripes to the cockroach's visual field. In freely moving behavioral experiments, similar stripe patterns consistently evoke turning. On the oiled-plate tether, mechanical linkage between legs is reduced or eliminated. Therefore, each leg can commence turning at different times. We, thus, established that turning occurred when the feet (tarsi) moved in a manner consistent with turning as established in previous studies (Mu and Ritzmann, 2005; Szczecinski et al., 2014). For example, stripes moving to the right should generate turns to the right. Those turns should include lateral extensions of the left front and middle legs (outside legs) and pulling movements of the right front and middle legs. Hind legs tend to either continue moving the same as they did in straight walking or stopped moving (inside leg) to create a pivot for strong turns.

Once each leg was determined to be in turn mode, we could then document the changes in joint kinematics that caused those changes (Szczecinski et al., 2014). As with straight walking, the joint changes for front and middle legs were very different even though the changes in foot trajectory were similar. For the middle legs, changes largely occurred in the femur-tibia (FTi) and coxa-trochanter (CTr) joints (consistent with previous findings (Mu and Ritzmann, 2005), while new data on the front legs showed that trajectory was altered largely due to changes in the three degree of freedom thorax-coxa joint (ThC) (Fig. 1). Indeed we were able to describe which of the three degrees of freedom were altered during turning movements (ThC2 increased joint excursion while ThC3 decreased). Because our tethered preparation and 3D joint kinematics system allows us to establish 3D joint kinematics of all joints in each leg simultaneously, we were then able to examine coordination among the various joints. We determined correlation coefficients for pairs of joints within legs and between legs. Not surprisingly, joints within legs were highly correlated. This finding is consistent with the model of joint pattern generators linked through inter-joint reflexes that has been established for stick insect (Büschges and Gruhn, 2008) and is the basis of our LegConNet control system. Recent findings in the Büschges laboratory strongly suggest that similar but weaker neural pathways occur between legs (Borgmann et al., 2009; Borgmann et al., 2007). We confirmed this notion also. Significant correlations existed between similar joints of legs that tend to move together in the same tripod. Finally, we found that within legs, groups of joints tended to shift in tandem in very reproducible but leg specific patterns when the insect transitioned from walking to turning.

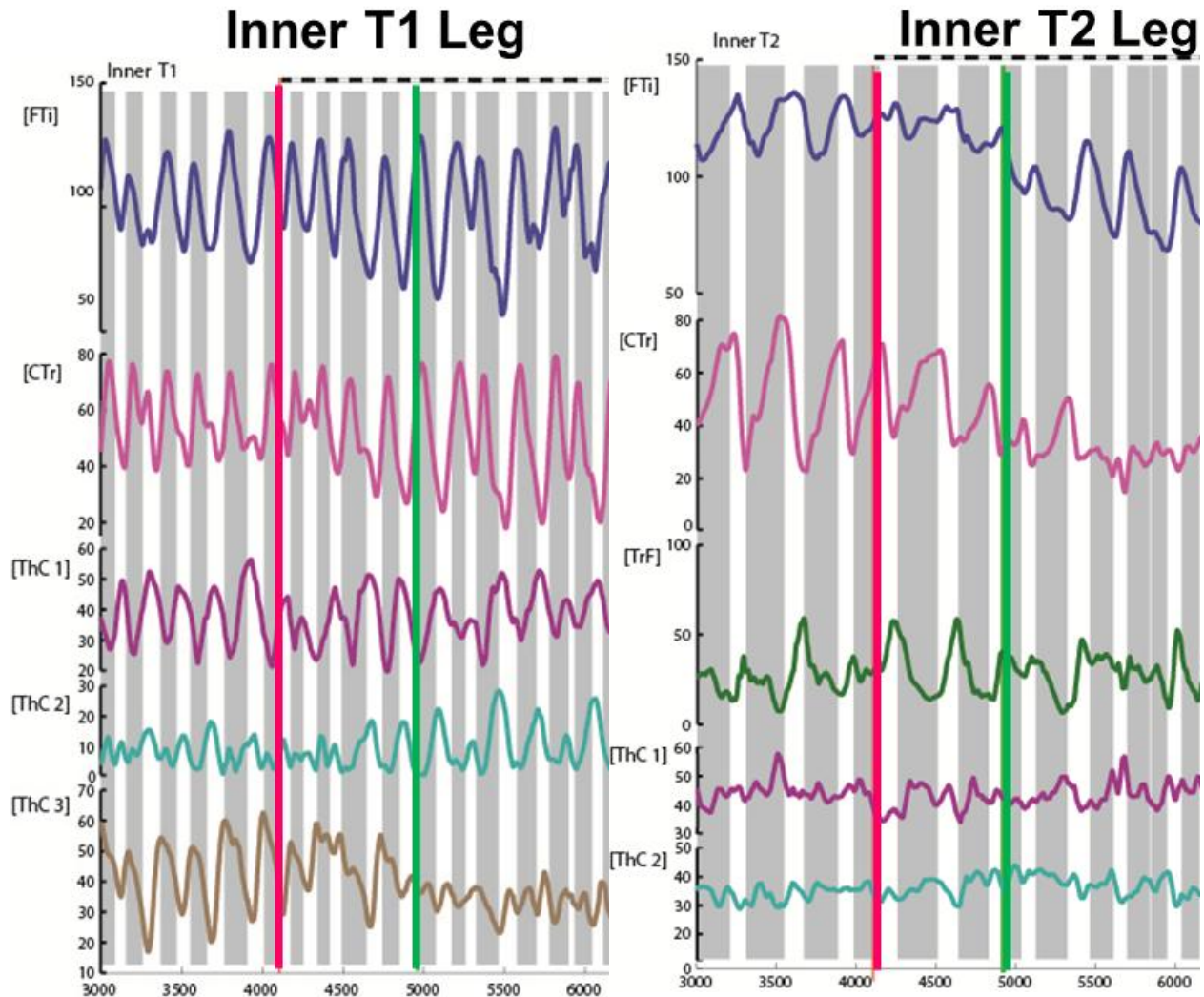


Figure 1: 3D joint kinematics of all joints of the T1 and T2 legs that moved on the inside of a simulated turning movement in a tethered cockroach. Although both legs switch from pushing the animal forward to pulling it through the turn, the joint movements that create these actions are distinct. The T1 leg relies heavily on actions of the second and third degree of freedom of the ThC joint (ThC 2 and ThC3) whereas in the T2 leg, these joints make little movement. Rather the changes in direction are accomplished by large changes in the FTi and CTr joints. Red line indicates time that a moving stripe pattern was turned on. Green line indicates time where turning movements commenced in that leg based upon the actions of foot direction. Shaded areas are stance phase for that leg. Note that because the oiled plate tether eliminates mechanical linkage among the legs, it is possible for each leg to move through different swing-stance cycles (as seen here).

These observations were used in tandem with what is known about insect locomotion to produce a neuromechanical model of the cockroach. It is known that insects possess a hierarchical control structure in which each joint has a basic controller that is subject to influence from within the leg, and then minor connections between the legs keep them in time (Akay et al., 2004).

In order to test our hypotheses about how descending information affects motor patterns, we needed to model the nervous system in this modular way. Therefore, each joint possesses its own central pattern generator (CPG), which naturally oscillates and generates the rhythm for each joint. It is known that these are not directly connected in the animal, but are coordinated into coherent motions (walking, turning, etc.) by shared sensory signals among the joints (Büschges et al., 1995). Sensory signals such as loading

Inner T1 Leg - Simulation

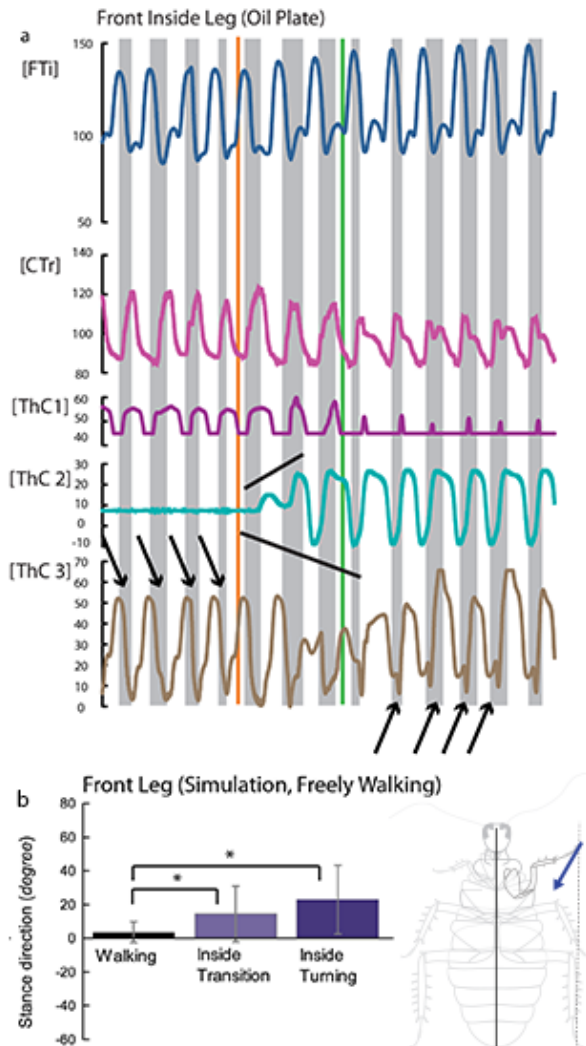


Figure 2: Joint kinematics from the front leg of our neuromechanical simulation of a cockroach. (a) We implemented a reflex reversal in the front leg on the inside of the turn that causes the ThC3 joint to change its phase, as seen in the animal. The orange line indicates time when a descending command to initiate turning was sent. The green line indicates time when turning movements commenced. Shaded areas are stance phase for that leg. (b) Graph showing the angle of the foot trajectory compared to forward motion. Implementing this hypothetical reflex reversal caused the model to generate foot trajectories that pulled inward along the turn, just as seen in the animal.

only does the ThC3 joint change its phase of motion, but it clearly alters the force vector applied by the tarsus of that leg to an inward pulling motion.

By modeling the networks of the animal at this level of detail, we can directly implement structures that are known to exist and make predictions about the animal. For instance, when our simulation was

information and joint angles are used to affect the timing of the neighboring joints and coordinate their phase.

Modeling this aspect of the system is crucial to test our hypothesis that the central complex can alter behaviors by modifying a reflex. For instance, for the middle leg to perform an inside turn, it must generate a pulling motion. Therefore it expects loading information at a different point of its stepping phase (during leg flexion rather than extension), so descending signals must change the pathway from the load sensors that normally cause FTi (the most distal joint) extension to cause flexion. In addition to reflex reversals, joints may change their excursion between walking forward and turning. Therefore, we expanded our model such that descending signals could also change motor neuron activation levels to change a joint's range of motion or bias it in one direction. Then for each leg, two neurons, one for reversing reflexes and one for changing joint excursions, can send simple, unpatterned signals to the joint controllers to transition the leg's motion from walking to turning. This supports our hypothesis, showing that this type of organization is plausible in a biologically realistic model.

We can then extend what is known about reflex reversals in general with our 3D kinematic data to construct a realistic model of how the animal's leg control networks may be organized. This is important because each leg of the cockroach (front, mid and hind) has different geometry and function, and our kinematic data revealed how each uniquely generates new motions during turning. For instance, we observed that ThC3 rotation changes phase in the inside front leg while the animal turns, suggesting that a reflex reversal like that in the middle leg occurs. We were able to validate this hypothesis in the model, showing that descending influences could change how sensory information is used by the low level control system to generate a new behavior from an established circuit. Figure 2 shows kinematic data from this transition. Not

allowed to walk freely in a simulated physics environment instead of walking as though on an oiled plate, the range of motion was higher in nearly every joint (Szczecinski et al., 2014). This suggests that the animal's motion may vary in small but important ways when allowed to move freely, motivating our experiments in which the animal is allowed to move freely.

Modeling walking networks as coupled CPGs also has the added benefit of making rhythms more robust. This improves both responses to perturbations to walking and the stability of transitions to turning. If not tuned precisely, our previous finite state machine implementation could cease stepping during the transition following a reflex reversal because it was dependent on sensory input to generate rhythm. Our CPG-based model, however, does not have this problem, because the CPGs enforce oscillatory motion at each joint, even if certain sensory cues are not obtained. In addition, extreme sensory signals, such as larger than expected leg loads, may abolish stepping because there is no mechanism for the system to escape the current state. However, our CPGs can in effect “time out,” forcing a transition to a new state, even when sensory signals are severe. We anticipated that adding a timer to our previous state machine would improve stability, and implementing CPGs has not only accomplished this goal, but done so in biologically accurate manner.

Alteration of Leg Movements by Descending Commands

Background: Ultimately, we would like to understand exactly how descending commands affect changes in walking behavior. Under our previous AFOSR grant, we demonstrated that local reflexes could shift sign as a result of descending activity. For example, relaxing a leg stretch receptor that monitors femur-tibia joint angle normally inhibits activity in the principle extensor motor neuron (Ds) of the coxa-trochanter joint. However, after eliminating all descending activity by cutting both neck connectives, relaxing this sensor now excites Ds (Mu and Ritzmann, 2008a). Similar studies on stick insect in the Büschges laboratory demonstrated that local reflexes switch sign when that insect walks backward (Akay et al., 2007) and when turning (Hellekes et al., 2012). Indeed these kinds of reflex reversals are the basis for transitions between forward walking and turning in the simulation that is described above (Szczecinski et al., 2014).

In order to further identify which brain regions generate descending commands that evoke such altered leg movement, we completed two studies examining the role of the central complex (CX) of the cockroach brain in altering stepping movements. The CX is a prominent group of midline neuropils found in virtually all insects. It has been suggested that it may play a role in supervising locomotion (Strausfeld, 1999). Large lesions in this region have serious consequences on the cockroach's ability to negotiate a U-shaped track (Ridgel et al., 2007). Moreover, the behavioral effect of more discrete electrolytic lesions varies with placement within individual CX neuropils. For example, lesions in the lateral region of the fan-shaped body (FB) have profound effects on turning, whereas FB lesions near the midline have little influence on turning, but instead altered climbing behaviors (Harley and Ritzmann, 2010). Neurons residing in the CX project to a bilateral pair of neuropils called the lateral accessory lobe (LAL). Descending fibers that are activated by various sensory systems and project to thoracic ganglia often pass through the LAL and lesions to the LAL typically result in failure to turn at all. The CX processes multiple forms of sensory activity (Ritzmann et al., 2008) and is also affected by neuromodulators (Kahsai et al., 2010) and ascending signals (Homberg, 1987) that may report on the internal state of the animal. With this information, we know that the CX can modify descending signals as they pass through the LAL in order to assure that they are consistent with current conditions. Under our previous AFOSR grant, we demonstrated that activity recorded extracellularly from the CX correlated directly with moment-to-moment changes in step frequency (Bender et al., 2010a). Indeed, some of these changes in CX activity *preceded* changes in step frequency, suggesting that they could be a source of descending commands. Consistent with this notion, stimulation through the same electrodes evoked changes in step frequency.

Brain recordings during tethered turning: Following upon these findings, our work under this AFOSR grant looked directly at the descending commands that arise in the brain and evoke changes in local control. For technical reasons, we decided to concentrate on the changes from straight walking to turning.

To examine this descending control, we implanted extracellular electrode wires in a tetrode arrangement into various brain regions and then recorded from or stimulated through the wires as the tethered cockroach walked on an air suspended Styrofoam ball (Guo and Ritzmann, 2013). In order to keep the behavior as natural as possible, turning was evoked by self-generated tactile stimulation of the cockroach's antennae. A bar was placed near the insect's head and when an antenna contacted the bar, the cockroach turned toward it. We then excerpted recordings from brain neurons as well as information on the ball's movement before and after antennal contact.

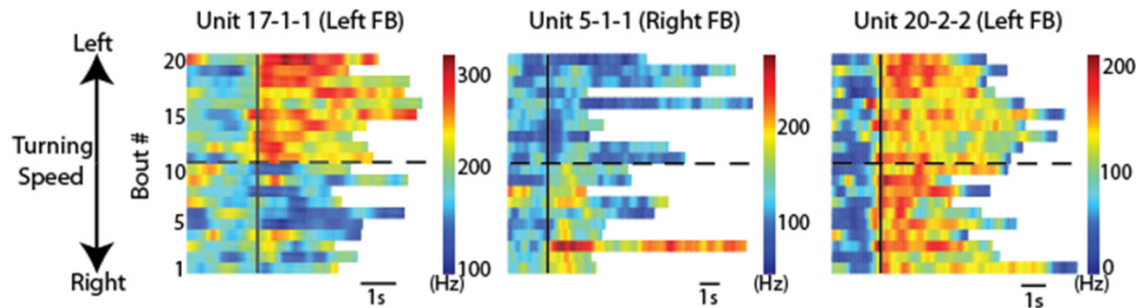


Figure 3. Activity recorded in three FB neurons associated with turning bouts. Turning was evoked by antennal contact with a post. Each row is one bout from each unit associated with left turns (above dashed line) and right turns (below dashed line). Note Unit 17-1-1 recorded in the left FB increases activity during left turns, while Unit 5-1-1 recorded in the Right FB increases activity only during right turns. Unit 20-2-2 increases activity to turns in either direction.

These recordings clearly show asymmetries in unit activity associated with contact with one antenna (Fig. 3). The activity immediately after antennal contact is compared to activity over a similar period prior to antennal contact. There is a spatial pattern of significant increases in CX neural activity that is associated with turn direction. Units recorded on the right side of one of the CX neuropils, the fan-shaped body (FB), showed significant increases only when the cockroach turned to the right, but *not* when it turned to the left. In some units, there was also an increase in activity associated with changes in forward locomotion. Units recorded in the left FB (data not shown) showed the opposite pattern, responding during left turns and in some cases forward walking but not during right turns. In contrast, units recorded in the middle FB were indiscriminate to turn direction, responding during turns in either direction as well as to forward walking movements. This pattern is consistent with previous results showing that electrolytic lesions only affect turning when they were generated in lateral regions of the FB (Harley and Ritzmann, 2010).

As with our analysis of CX unit activity associated with changes in walking speed (Bender et al., 2010a), we also compared instantaneous firing rate of each recorded unit to the speed of turning or forward walking as measured, in this case, by monitoring the speed of the ball tether's rotation (Fig. 4). The same pattern emerged as that seen in figure 3. Instantaneous firing frequency of units recorded in the right FB were strongly correlated to right turning ball movement but not to left turning or forward walking. In contrast, firing frequency curves of units recorded in the middle FB were strongly correlated to ball movement in either direction or to forward walking responses. Stimulation through the same electrodes also evoked turning movements.

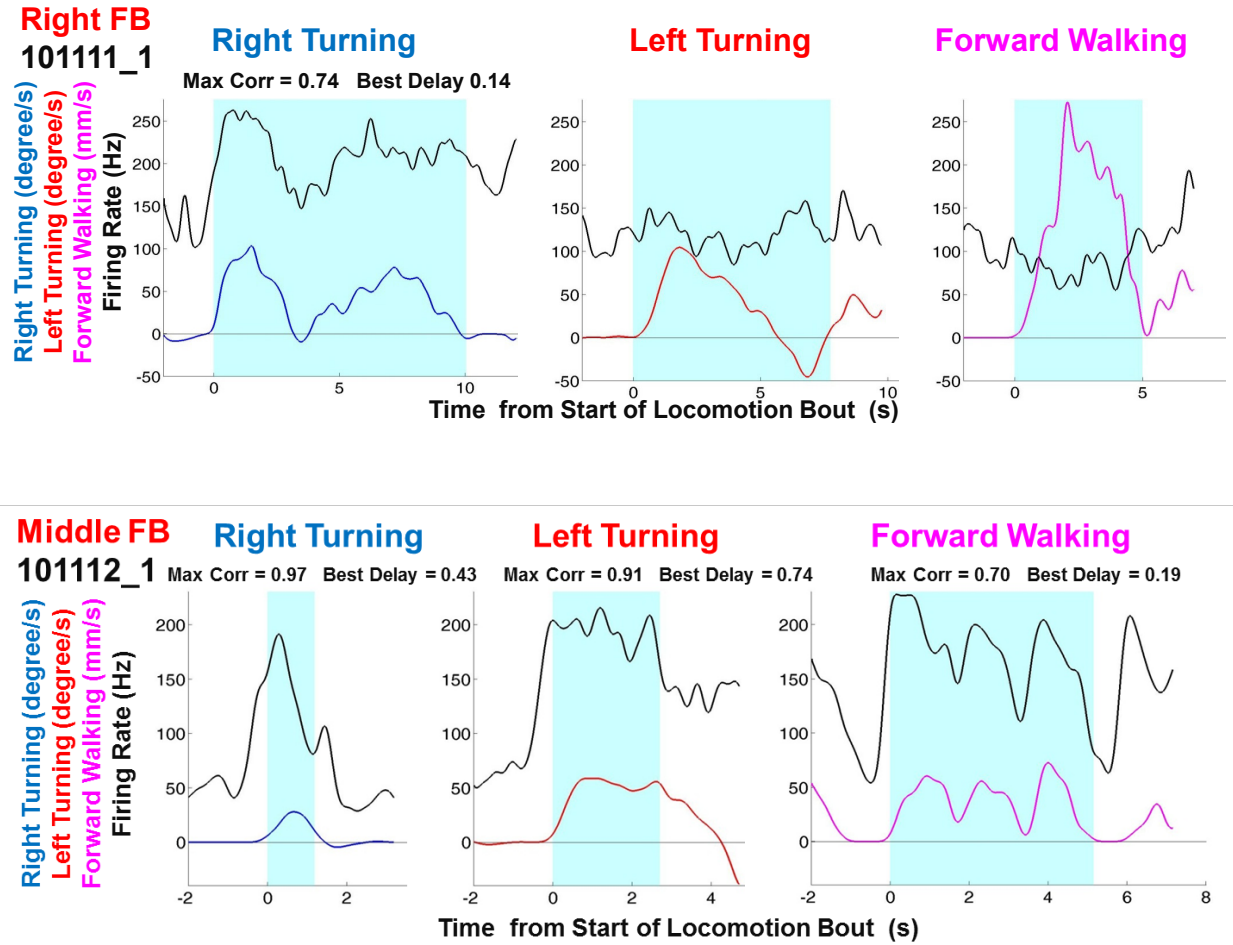


Figure 4: Instantaneous frequency individual bouts recorded for the two units shown in fig 2 along with traces of right, left and forward movement of the ball. Consistent with the pattern in fig. 2, the activity pattern of the unit recorded in Right FB was strongly correlated with ball rotation during right turns, but not during left turning or forward walking. In contrast the activity pattern of the unit recorded I the middle FB was correlated with all forms of movement.

The tuning of individual CX neurons relative to directional movement was documented in the following manner. The activity of the neurons was plotted simultaneously along with the forward walking speed and left-right turning angle. These records were then divided into bins (Fig. 5A). For each bin a vector was created from the forward and left-right turning movements (Fig. 5B). The vectors pointed from a 0 point at the origin of a two dimensional graph to a location along the Y axis (forward walking speed) and X axis (left-right turn angle). A square at the tip of that vector was then filled in with a color coded to the activity level of the neuron at that point in time (Fig. 5C and D). The result is a tuning graph as shown in figure 5D.

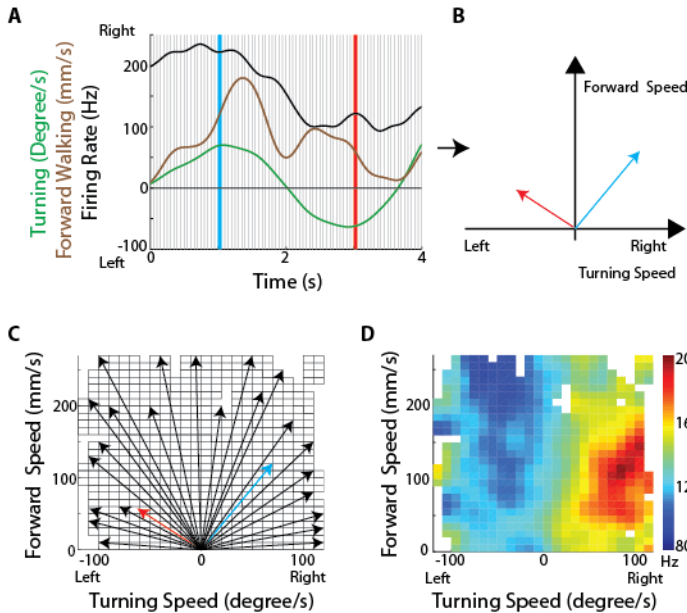


Figure 5: Methodological concept for generating firing rate maps. (A) For every recording session, forward and turning speed as well as spike times of each unit were smoothed using a Gaussian kernel with a standard deviation of 150ms. Each recording session was divided into non-overlapping 50ms long sections (between individual gray lines). (B) For each divided section, a velocity vector was generated by averaging forward and turning speed within that period. Firing rate for each velocity vector was also calculated. The blue and red vectors were obtained from the blue and red lines, respectively, in A. (C) All velocity vectors were binned into a forward walking speed versus turning speed graph (10 forward walking speed and 10deg/s for turning speed). Only some of the vectors, including the two vectors in B, are shown here. (D) A firing rate map was generated by overlaying the averaged firing rate for each bin, obtained by averaging all the firing rates whose corresponding velocity vectors fell into that bin.

These motion-tuning graphs resulted in patterns that again were correlated with position within the CX. As with the linear displays in figure 3, we see here units on the left side of the FB that are tuned to left turning and either slow (Fig. 6A) or fast (Fig. 6B) forward motion, neurons on the right side that are tuned to right motion and other units just tuned to forward fast motion (Fig. 6C) which were found throughout the FB. Stimulation through the same electrodes generated turns that were consistent with these recordings (i.e. stimulation on the right side generated turns to right and vice versa).

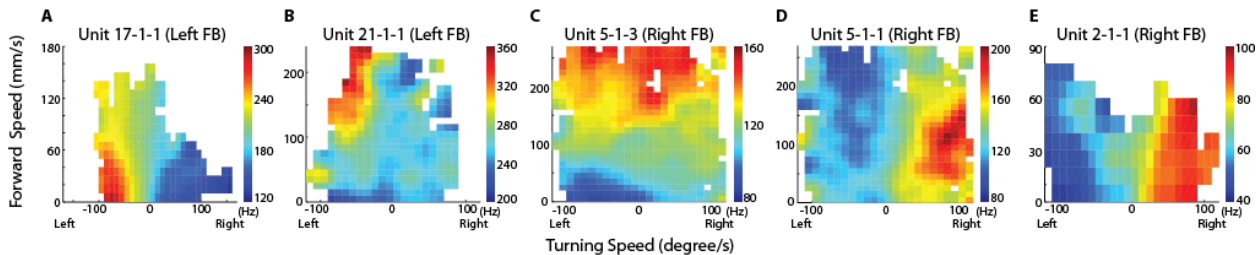


Figure 6: CC units are tuned to self-motion. Firing rate maps for locomotion initiated by antennal contact with the rod for representative CC units. The x-axis is the turning speed and the y-axis is the forward walking speed. Positive turning speed indicates right turning and negative turning speed indicates left turning. CC units showed discrete locomotion-related firing fields, such as left turning irrespective of forward walking speed (A, $Z=3.59$, $P<0.01$), forward walking to the left (B, $Z=4.08$, $P<0.01$), forward walking irrespective of turning speed (C, $Z=5.73$, $P<0.01$), forward walking to the right (D, $Z=6.00$, $P<0.01$), and right turning irrespective of forward walking speed (E, $Z=2.33$, $P<0.01$).

Movement in an Arena: Data that our laboratory has obtained over several years, such as that described in the previous section, point to a role for central complex (CX) neuropils in decisions made by cockroaches as they navigate complex terrain (Ritzmann et al., 2012). Our behavioral data demonstrate that mechanical antennal information along with visual cues guide these decisions as the cockroach walks through a track and encounters a barrier (Harley et al., 2009). These types of sensory cues are processed in CX neuropils where units are found whose activity appears to influence locomotory changes (Bender et al., 2010a; Guo

and Ritzmann, 2013). Moreover, both permanent and reversible lesions in the CX have dramatic effects on these same behaviors (Harley and Ritzmann, 2010; Kathman et al., 2014).

These results strongly support the notion that activity descending from the CX interacts with local control circuits in the thoracic ganglia to re-direct leg movements. For this reason, we proposed to observe cockroach behavior in a much more enriched situation. Under our AFOSR and NSF grants we developed a 90cm by 90cm arena that can now be used for a range of experimental protocols that examine the mechanisms that we identified under more restricted situations now in ever more complex environments.

Some turning behaviors clearly do not require direct control by the brain. For example, escape responses rely on wind sensors on the rear of the insect and involve primarily thoracic circuits (Ritzmann and Eaton, 1997). The difference between the behaviors that are associated with direct connections of sensory interneurons to thoracic motor circuits and the kinds of behaviors that the CX is involved in may be temporal. Escape movements or even rapid wall following must occur in the millisecond range. But foraging decisions that dominate most animal behaviors can occur over much longer time frames. A study of walking speeds in a large arena demonstrated that cockroaches spend most of their time walking relatively slowly around in their environment exploring with their antennae while taking in tactile, visual and olfactory cues, and then moving accordingly (Bender et al., 2011). Indeed, walking speeds in that arena clustered around two speeds (Fig. 7); a slow ambling gait (<10cm/sec) and a less common faster trotting gait (~30 cm/sec). Even these trotting gaits occurred at speeds well below the median escape velocities recorded in the open arena (41.1cm/sec). A breakdown of the time that the cockroaches spent moving at these different speeds showed that when they were near the wall of the arena (their preferred location), most of their movements were in the slowest range. When they were in the middle of the arena, they often changed to the faster trotting gait, presumably to get back near a wall. Thus, the cockroach spends most of its time moving slowly through its environment examining objects and reacting accordingly. The rapid movements associated with escape are, in fact, rare occurrences that occur only in the face of an imminent threat. So, while there is no question that these rapid behaviors are critical to the cockroach's survival and are very useful experimentally in working out reduced neural circuits and biomechanical properties (Jindrich and Full, 2002; Koditschek et al., 2004), we need to appreciate the relatively small part they play in the insect's behavioral life.

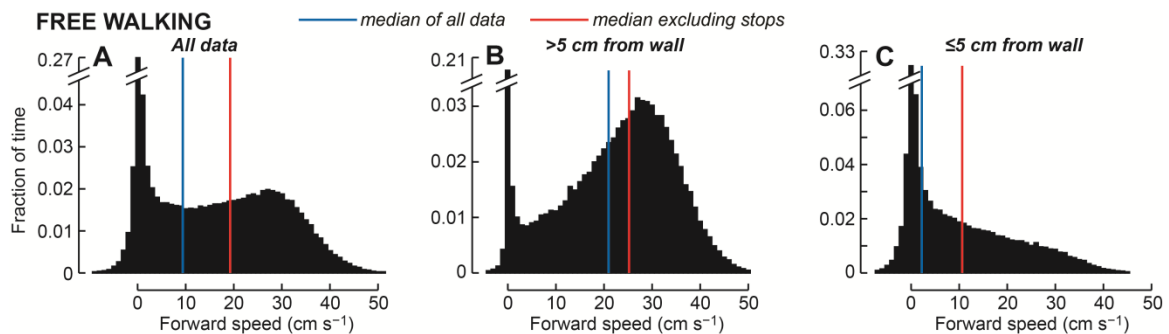


Figure 7: Forward walking speed in the open arena. (A) Pooled histogram from 44 animals, ~1 min of walking each at 20 samples s^{-1} . (B) Speeds when the animal was more than 5 cm from a wall, approximately the radius of antennal contact ($n=31200$ samples). (C) Speeds when the animal was less than 5 cm from the nearest wall (panel A – panel B; $n=28464$ samples). The blue vertical lines indicate the median walking speed in each histogram; the red lines show the median speed when data with an absolute value less than 1 $cm s^{-1}$ are excluded. From Bender et al., (2011).

In our first behavioral task, we allowed cockroaches to seek a darkened shelter in the arena, sometimes partially blocked by a transparent wall. Most cockroaches (including *Blaberus*) are extremely photonegative (Canonge et al., 2009; Meyer et al., 1981; Okada and Toh, 1998), and thus the dark shelter attracts the animals in about half the time than would be expected based on control trials in an empty (no shelter) arena (Tietz et al., 2011). However, as noted above, they are also known for thigmotaxis (Halloy et

al., 2007; Nishiyama et al., 2007; Okada and Toh, 2006), spending much of their time along the walls of such arenas while relying on antennal contact to maintain a constant wall proximity (Camhi and Johnson, 1999; Cowan et al., 2006). Thus, as was the case in many of our simpler behavioral situations, there are multiple sensory systems that, by themselves, would control much of the cockroach's behavior. Thigmotaxis would dictate staying on the wall while photonegative tendencies would have the cockroach leave the wall and move directly to the shelter. How are these seemingly conflicting behaviors resolved? Is an environmental map required? Does the cockroach brain plan the best paths? Can the total behavior of the animal be modeled as a series of mono-sensory reactions?

To begin to answer these questions, we observed many individual cockroaches in the arena to develop a model of their shelter-seeking behavior (Daltorio et al., 2012; Daltorio et al., 2013). When a wall was encountered, the insects generally followed it. Occasionally, they changed direction along the wall or departed the wall to explore the interior of the arena. We fit the insects' continuous turning within the arena to a Biased Persistent Random Walk. How these parameters vary with the perception of the shelter defines our model, RAMBLER (Randomized Algorithm Mimicking Biased Lone Exploration in Roaches). In a simulation we demonstrate that the following trends found in the animal tracks were sufficient to capture much of the shelter-seeking bias:

- 1) Change turn direction more often if the insect is turning away from a darkened shelter
- 2) Turn less often when facing a darkened shelter
- 3) Change direction on the wall less often when facing a darkened shelter
- 4) Depart wall more frequently if shelter is behind the insect

The level of complexity of the RAMBLER algorithm is an indication of the multi-sensory dependencies we expect to find in the insect's brain. The animal is neither blindly wall-following nor perfectly tracking the goal. When wall-following, the animal is more likely to depart when the shelter is behind it. This shows that even while relying on antennal feedback to maintain the proper wall-following distance, the insect is evaluating the changing visual response to decide when to leave the wall. When the antennae are not in contact with the wall, the turns the insect makes may at first glance appear random. However, our analysis shows that when the shelter is in front of the cockroach, it turns away less frequently and is more likely to correct turns away from the shelter. The presence of a visual goal seems to modify the normal turning and wall-following behaviors to correct for undesirable changes in the animal's perception. It is interesting to note that this model required little memory and we find no evidence that the cockroach is planning its route. Eventually, the cockroaches almost always reach the shelter, but they do not always stay there. They may leave and return several times. This observation in itself suggests that the cockroach is not dominated by a single-minded goal to reach the darkened shelter, but rather is continuously considering several factors as it moves.

Brain recording in freely moving cockroaches: We next combined our brain recording efforts with the arena experiments to record from the CX in freely moving insects. We adapted the tethered brain recording technique to use in free ranging subjects (Guo et al., 2014). We could then record from units while the insect moved around the arena (Fig. 8). The color coded trace in figure 8B shows the activity of a single unit as the insect moves about the arena.

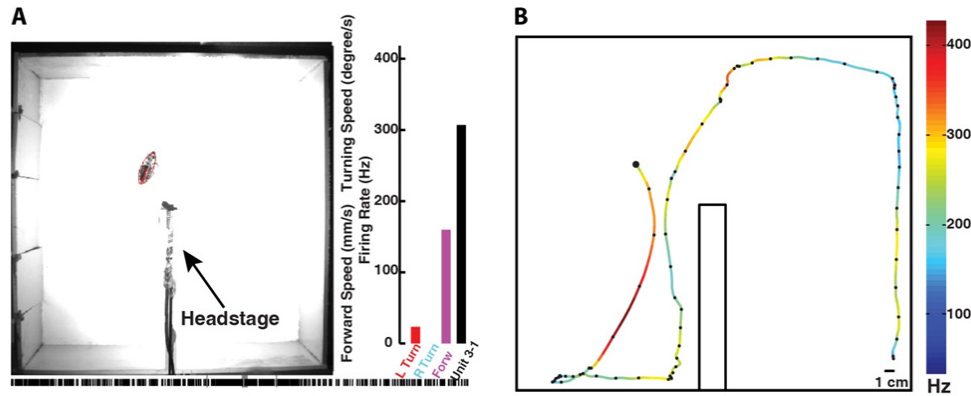


Figure 8: Neural activity recorded in freely moving cockroach. *A* Photo of cockroach (red outline) in arena. *B*. Track of cockroach movements with activity in unit 3-1 color coded according to bar at right.

We then generated motion-tuning graphs for these units (Fig. 9) as we did for the tethered experiments. However, we extended this analysis to allow us to compare motion-tuning among CX neurons in several subjects. To accomplish this goal we first smoothed the motion-tuning graphs, then generated contours that represented activity levels ranging from 0 to maximum activity. The mid-range (50% contours) could then be compared to other units. Examples of nine categories of 50% contours from several subjects are shown in figure 9. Clearly the same patterns are seen in different neurons from various individuals.

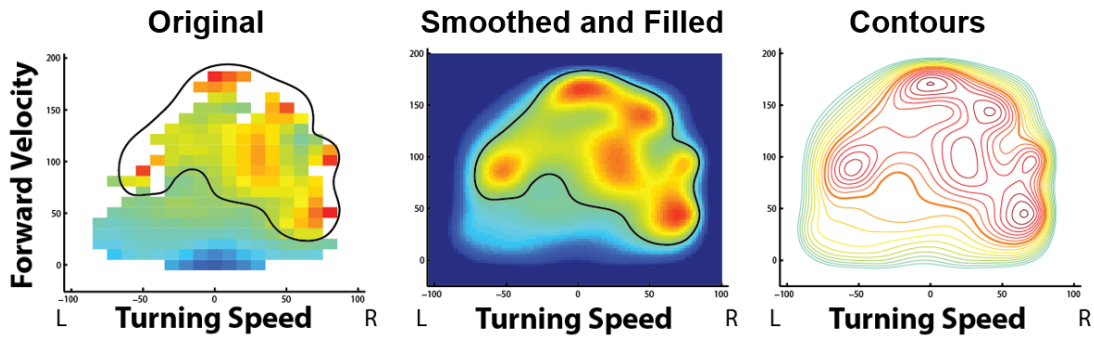


Figure 9: Generation of contours depicting activity of units in freely walking insects regarding turning and forward walking speed. The original graph is smoothed and the contours depicting the range of activity levels from 0 to maximum (100%) are fitted to the smoothed surfaces.

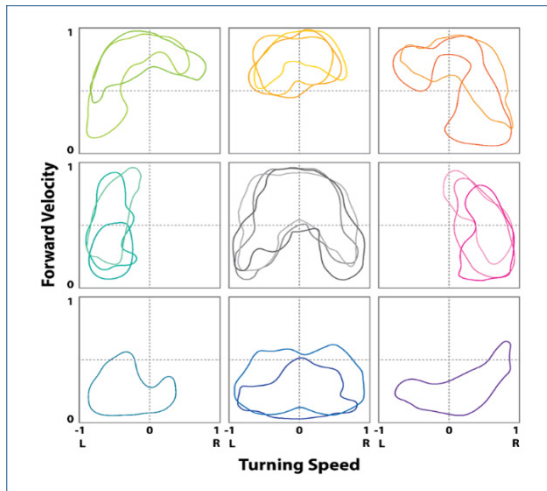


Figure 10: Nine types of 50% contours generated as in fig. 9 for neurons recorded from several different insects.

CX activity was also monitored in freely moving cockroaches as they climbed over blocks. Here we found increased activity in many units preceding upward movement. In contrast to turning CX units, climbing units were often recorded on the brain's midline. To quantify this effect, we took advantage of our earlier finding that activity in many CX units are highly correlated with step frequency. We plotted activity against walking speed and isolated those bouts of leg movements that were associated with climbing versus those during walking (Fig. 11). While some units maintained the same walking speed relationship while climbing (e.g. Cells 3.1, 14.2 and 15.1 in figure 11), others were significantly elevated (e.g. Cell 15.1) or had their slopes change (e.g Cells 6.1 and 13.2) suggesting a change in state preceding the climbing movement. An alternative explanation is that the CX neurons were elevating their firing rate in response to increased load as

the insect pushed upward. To test this possibility, we doubled the mass of the insect by adding weights (Cell 15.1 in figure 11). There was never a change in the activity vs. step frequency relationship with this increased mass that was high enough to account for the changes associated with climbing.

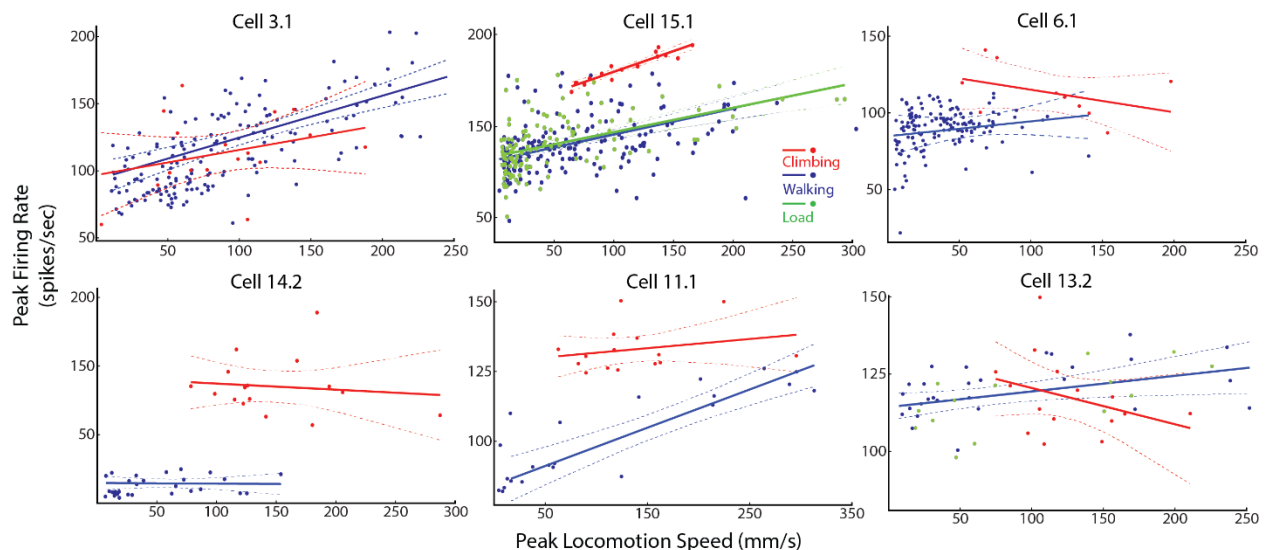


Figure 11: Firing frequency vs. walking speed for 6 units taken from cockroaches climbing over a block. Blue dots and lines are bouts of walking on flat surface. Red dots and lines are during climbing. The green dots and line for Cell 15.1 is taken from an insect walking on a flat surface while dragging a weight that doubled its mass.

Reflex State Changes associated with CX Activity: The final step in our proposed work was to establish how the CX effected changes in the leg movements. To examine this mechanism, we followed up on the previous observation that reflex activation of motor neurons reversed when neck connectives were severed, thereby eliminating any descending commands (Mu and Ritzmann, 2008a). In normal intact cockroaches stretch of femoral chordotonal (FCO) evokes a resistance reflex in the motor neurons that extend the FCO and relaxation terminates that activity. However, it also activates the extensor motor neurons (Ds) of the next proximal joint (the coxa-trochanter joint) during stretch and inhibits that neuron during FCO relaxation. These inter-joint reflexes are known to be critical to coordination of leg joints and as the insect changes direction of leg movement, they are known to reverse (Hellekes et al., 2012). Likewise, lesion of

neck connectives causes a reversal of these inter-joint reflexes that is particularly clear during relaxation, when Ds switches from inhibition to excitation (Mu and Ritzmann, 2008a). Such reversals were also generated in some cases as a result of discrete electrolytic lesions within the CX. This led to the hypothesis that CX activity affected descending commands that could manipulate such reflexes, thereby, re-directing leg movements.

To test this hypothesis, we selected cockroaches that showed CX activity that was correlated with turning and whose electrodes could generate turning. Those individuals were moved to a restrained setup for testing reflexes generated by moving the FCO. We could then stimulate the same CX electrodes while the FCO was stretched and relaxed. Consistent with our hypothesis, stimulation at brain sites that were correlated with turning also reversed FCO reflexes in a manner consistent with changes in joint angle during turning (Fig. 12) (Martin et al. *in preparation*).

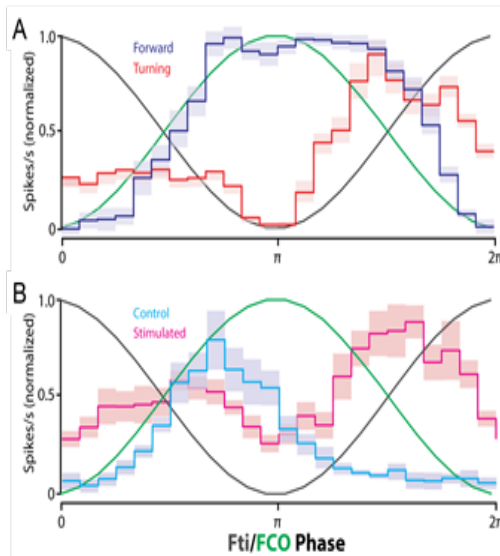


Figure 12: Reversal of FCO reflex parallels motor changes in turning. *A.* Ds activity is shown during walking (blue) and turning along (red) with FTi angle (black line) and FCO phase (green line). Note increased activation switches from occurring during FTi flexion (FCO stretch) to FTi extension (FCO relaxation). During forward walking, the activity remains high throughout stance probably due to activation of load receptors after touchdown. In the isolated reflex preparation (*B*) a similar reversal occurs from the control situation (blue) with Ds activation during FCO stretch and no activation or inhibition during relaxation to Ds activation during relaxation during CX stimulation (red).

Future considerations – State dependent stalking behavior: As successful as the cockroach experiments have been during the life of this grant and will continue to be in the future, there is a limitation to cockroach experiments. While we can predict that the cockroach will turn when encountering certain objects as well as the turning direction, we cannot predict the exact angle of the turn. This kind of question can only be addressed in an insect that is making a precise targeting movement such as that done by predators. For this reason, we have begun to turn some of our attention to a close relative of the cockroach, the praying mantis. Both of these insects are in the order Dictyoptera and have similar head, brain and body plans. However, mantises are very aggressive predators. They stalk prey (cockroach nymphs) and ultimately strike them with their forelimbs. The stalking behavior is very precise as is the strike.

Having completed the walking biological aims on the grant, over the last year we moved to transition our techniques to the mantis. These efforts have paid off tremendously. We can now record from the mantis CX during tethered or free walking behavior including stalking and strikes. We have also developed a gantry apparatus that follows the mantis as it moves carrying two high speed cameras for continuous 3D close up high-speed video of the behavior. Finally, we developed an arena that has an LCD computer screen on the floor. The computer can then generate moving squares on the LCD that the mantis will readily track and strike at. Thus, we can provide very controlled targets and decoys to the mantis while we record from its CX.

Preliminary experiments have been very exciting. For example, one neuron recorded during an encounter with two different cockroach nymphs revealed remarkable properties.

At the outset of the experiment, the mantis was exploring the arena looking for prey. As with our earlier cockroach experiments, this neuron increased firing activity just before the mantis's turning or rapid stepping actions (Fig. 13A). However, once the mantis locked onto a cockroach, the neuron "switched its attention". It now increased activity along with movements of the prey (Fig. 13B). In this case, the nymph escaped. However, shortly thereafter, the second nymph which was on

its back began struggling. At this point, the mantis turned its attention to that individual and this same neuron increased activity in concert with that prey's struggling movements (Fig. 13C). If the nymph ceased moving, the neuron went silent, but then increased again when the nymph began moving again while the mantis stalked in and finally struck the prey. During this sequence the first nymph moved through the mantis's field of view but was ignored as the mantis now concentrated on this new target. Thus this recording demonstrated a neuron that was correlated with the mantis's own movement but switched to prey as the mantis attended to first one and then another prey as it stalked and eventually attacked this second target.

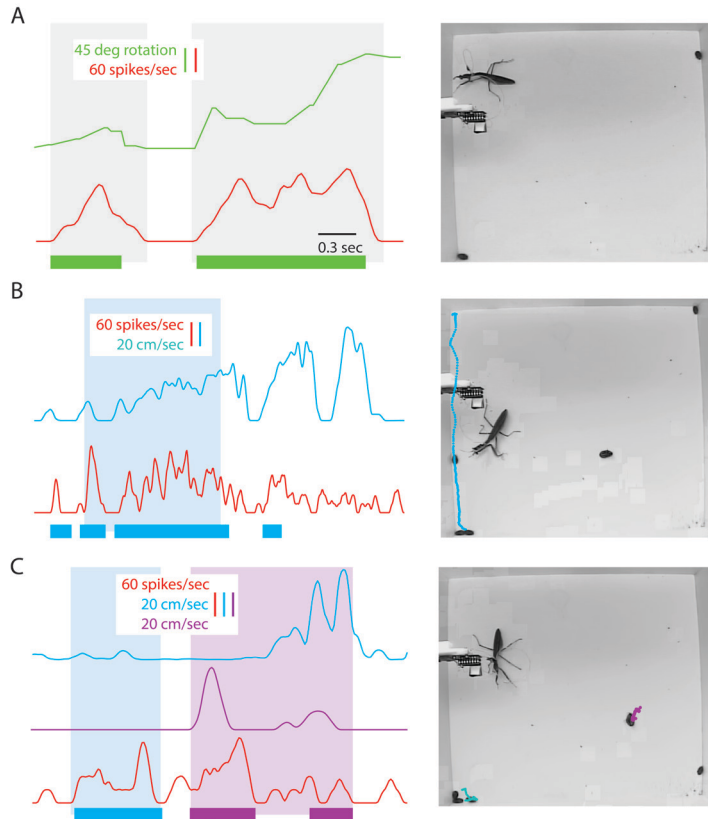


Figure 13: Activity in a CX neuron recorded in the brain of a praying mantis as it stalks first one and then another cockroach nymph. In all cases red line is the activity of the CX neuron vs time. Color coded bars under each graph indicates periods when the neural activity is correlated with the action of the same color with a correlation coefficient of ≥ 0.7 . A. Green line shows rotation of the mantis's body correlated with the neuron's activity. The shaded region marks frame when the mantis is making slow leg movements. Here as in the cockroach recordings the neural activity slightly precedes movement. B. The mantis sees a moving cockroach and begins to stalk it. The shaded region of this figure marks periods where the mantis is pointed toward the prey. At this point the activity of the same neuron is highly correlated with the prey's movements as it runs along the wall (blue track in frame next to graph). There is still a small correlation with mantis movements (not indicated here). Activity now occurs slightly after the prey movement. The correlation becomes reduced as the roach moves away. C. The mantis is still oriented toward the first prey for a short time, but then notices a second cockroach nymph that is on its back and struggling. Here the shaded region marks the time during which the mantis faces the prey and the prey is struggling. Activity in the same mantis neuron now is correlated with this second prey's movements until it stops struggling at the end of the magenta shading. Note that the first prey that the mantis is no longer attending to makes a strong movement at the end of the magenta shaded region, but the mantis neuron is no longer correlated with that. Eventually, the second prey began to struggle again and the mantis completed its stalking and eventually struck and consumed it. The neuron's activity was correlated to the remaining stalking movements (not shown) but not the actual strike.

We have also found that this species of mantis (*Tenodera sinensis*) alters its predatory behavior when it feeds. A starved mantis will actively stalk prey for some distance. However, as it feeds the number of steps it will take in the hunt decreases. Ultimately, it switches to an ambush strategy. Remarkably, this same switch can be evoked by injecting insulin into the hemocoel of a starved mantis.

With these preliminary results, we have submitted a renewal proposal to the AFOSR to examine the CX population activity under changing physiological state. Taken with our previous cockroach data, we hypothesize that the mantis keeps the prey in front of it as it approaches by turning behaviors associated with activation of lateral FB neurons. When the mantis stalks and approaches the prey, the population code found in the CX columns increases ultimately triggering a strike. As it feeds, neuromodulators associated with insulin reduce the size of this population code reducing the tendency to stalk but retaining the strike should the prey get close enough on its own. We believe that we currently have the tools necessary to examine this hypothesis. A successful test of it will greatly increase our understanding of hierarchical control of state dependent targeting and stalking behaviors in these animals.

Development of Hardware Models of Insect Leg Control

Background: Our previous leg controller network (LegConNet) and that originally done by Ekeberg in simulation (Ekeberg et al., 2004) were models implemented as augmented finite state machines. Also, the joint controller actions were switched entirely by sensory events rather than internal excitation. Büschges has shown uncoordinated cyclic joint motions in a deafferented stick insect leg indicating that the joints have independent CPGs that are influenced by inter-joint sensory activity (Büschges, 1995). We departed from our previous work in two ways. First, we integrated simple joint CPGs with the finite state controller network so that at low speeds the joint oscillators were sensory driven as before and at higher speeds they transitioned to sensory modulated CPGs. Second, we developed a biological neural network (BNN) model of the leg controller that includes the sensory pathways identified in the insect and CPGs at each joint. We also developed a new robotic cockroach leg model that includes additional motor and load sensors that more closely model sense organs found on the animal, which were necessary for our planned experimentation. Furthermore, we have changed our software implementation to real-time LabVIEW, which has several advantages including an easily reconfigurable Graphical User Interface and easier transitioning to other researchers.

Addition of Strain Gauges to Model Campaniform Sensilla in a Cockroach Leg Model: The cockroach leg model has been modified to include strain gauges that model campaniform sensilla on the trochanter segment. Sasha Zill, Professor at Marshall University, has done extensive work on the effects of campaniform sensilla on walking (Zill et al., 2004) and was excited to work with us on a series of experiments to determine how positive load feedback is used to generate adaptive walking. We, in turn, have included this information into our controller.

Campaniform sensilla (CS) are sensory neurons whose dendrites insert into a cuticular cap on the exoskeleton (Fig. 14). The elliptical geometry of these caps is such that they deflect, thus producing activity in the neuron, when the exoskeleton experiences compressive strain on its minor axis. Arrays of CS are situated in very specific areas of large strain on the trochanter and have a combined response that is proportional to the amount of strain in the exoskeleton. The CS are also arranged such that specific groups respond to strains that are either perpendicular to or in line with the leg-plane formed by the trochanter and coxa segments. Strains in the trochanter exoskeleton can be caused by both external forces on the leg or by joint torques and CS response is proportional to the sum of the two.

Strain gauges used to model the CS were placed on the robot leg's trochanter as close to the CTr joint as possible, the position of maximum strain (Fig. 14). They are placed on perpendicular sides of the trochanter to reflect the directionality of the CS. Initial experiments classified the effects of static loading on the robot leg. As seen in Fig. 15, the strain gauges responded linearly to external loads on the distal part of the trochanter, torques at the CTr joint, as well as combinations of both. To test the directional response,

weights were hung from the distal end of the trochanter and both strain gauges were monitored as the trochanter was rotated 360 degrees. The responses from the strain gauges were sinusoidal and 90 degrees out of phase with one another. These results correspond to those seen in cockroaches and stick insects (Klein et al., 2011).

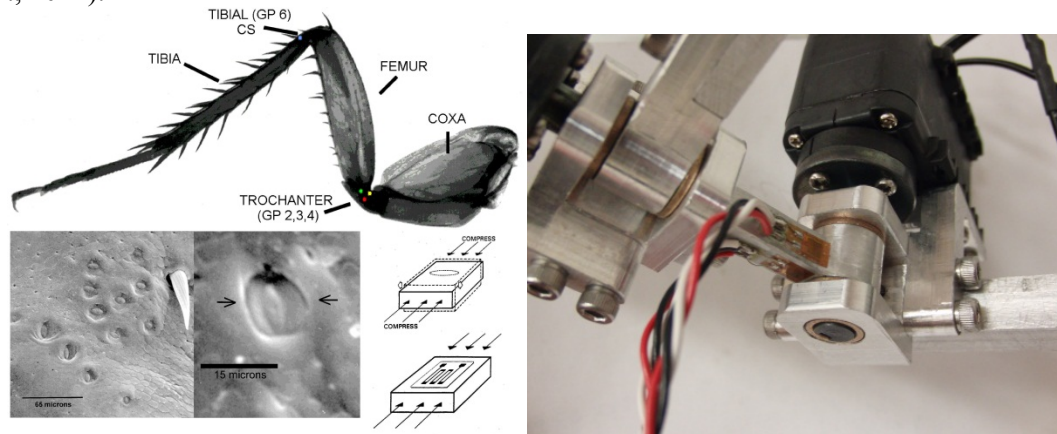


Figure 14: Two strain gauges placed on the trochanter near the CTr joint (right) are able to obtain sensory information that is encoded by four groups of campaniform sensilla on the cockroach (left). Campaniform sensilla consist of cuticular caps in the exoskeleton whose deflection corresponds to strain in the exoskeleton (left bottom).

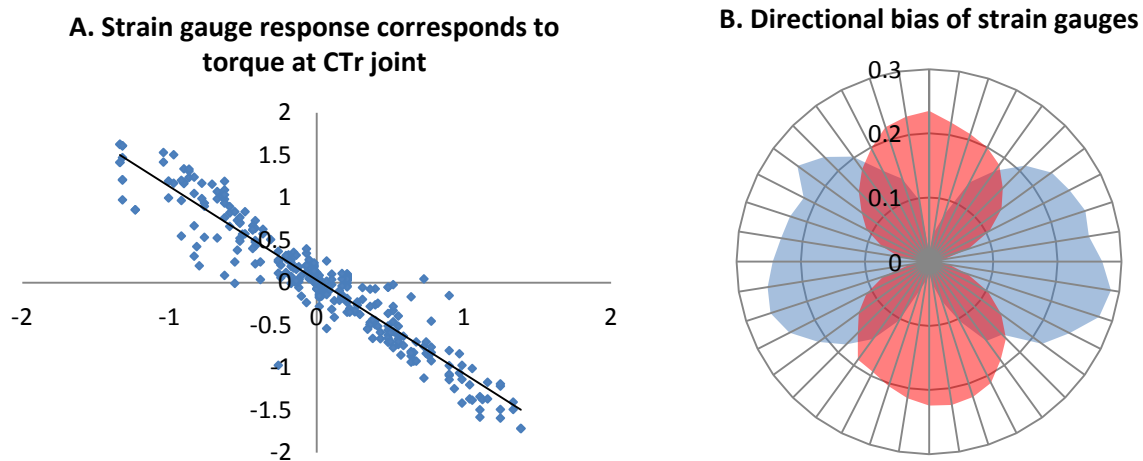


Figure 15: A.) External forces were exerted on the distal end of the trochanter while the CTr joint was fixed. Meanwhile, simultaneous measurements were taken from the strain gauges and from the torque sensors at the CTr joint. This shows the effectiveness of the strain gauges to encode the torque about the CTr joint. B.) Readings from the ventral strain gauge (red) and the anterior strain gauge (blue) as the trochanter is rotated 360 degrees with a weight hanging from the end. The strain gauges break the force into perpendicular components.

Our original LegConNet algorithm used sensory information to switch between states in a finite state machine in order to determine joint actions. However, previous robot legs had no way to sense strain in the trochanter segment, which is known to play an important role in modulating motor activity in the CTr joint (Zill et al., 2004). Instead, load was inferred with a simple switch on the foot or through motor activity. Strain measured in the trochanter segment of our new leg is a continuous value and has been incorporated into the LegConNet algorithm. Stepping activity was achieved using this approach and two steps can be seen in figure 16. The strain information differs from the ground contact sensor in that it is not Boolean but, rather, proportional to the load on the leg. Thus, it can be used to continually modulate muscle activity

during stance as the load changes, a phenomenon which is supported by experiments performed on the cockroach (Zill et al., 2004).

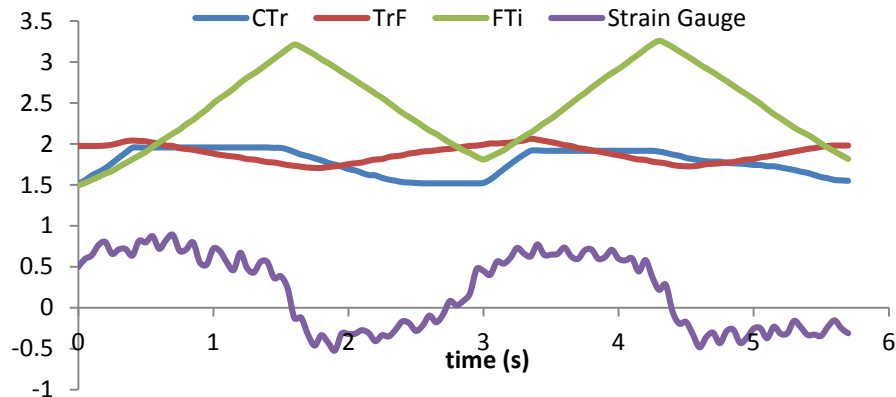


Figure 16: Data from two steps of the robot leg using the sensory based LegConNet. Joint angles are measured in radians and the strain gauge is calibrated to indicate torque about the CTr joint in $N*m$.

Graphical User Interface and Analysis Tools: This iteration of the robot leg is controlled using the LabVIEW programming language in conjunction with a National Instruments cRIO controller. Regardless of which particular algorithm is being used to control the leg, there are many control parameters which are interesting to adjust in experiments. LabVIEW has an intuitive graphical user interface (GUI) which gives the user real time access to all of the variables and parameters. This capability was one of the major aims of our project and is critical for the hardware model to be useful for biological hypothesis testing. Data can be displayed in real time through a graph or a number of different numeric outputs. Data are also output to a spreadsheet file along with synchronized video of the leg for later analysis. Examples of the GUI and experimental setup can be seen in figure 17.



Figure 17: LabVIEW GUI. Various parameters can be controlled in real time during locomotion experiments. Data are displayed in real time and saved to a spreadsheet for later analysis.

The advantage of testing hypotheses on the robot model instead of the actual cockroach is that we have access to all kinematic and sensory data, as well as all the variables and parameters of the neural network, at all times. This results in an overload of data that is at times difficult to analyze. At the request of biologists in our group, we have created a tool to replay and review previous data sets from locomotion experiments. The program seen in figure 18 allows the user to replay in real time or scroll through at any pace the locomotion of the model insect leg. As the data are displayed on the screen the recorded video of the leg motion can be reviewed to see what physical perturbations correspond to interesting data points. This is particularly useful when looking at the states of different neurons as different parameters are adjusted or the response of strain gauges during the transitions between stance and swing or external perturbations.

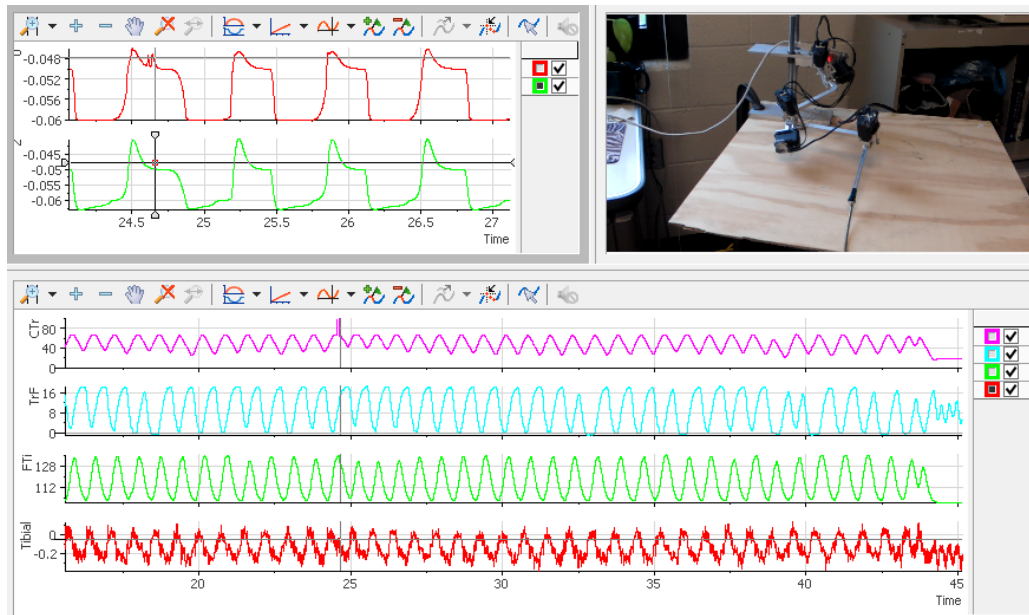


Figure 18: Sample playback GUI. This can be customized to play back any data set while simultaneously moving the robot leg accordingly.

A biological neural network implementation of LegConNet: Our finite state machine LegConNet gave insight into sensory coupled motor actions to coordinate joints within a leg into walking or turning patterns. However, it had shortcomings and biological simplifications that we sought to rectify, so we developed a neural model to address these. LegConNet approximated the continuous neural system of the animal as a discrete state machine. However, this limited the amount of analysis that could be performed to predict its behavior. Therefore, a biological neural network simulation is a more useful modeling tool (Daun-Gruhn and Büschges, 2011). In addition, LegConNet needed special cases and timers to ensure that it maintained periodic motion. CPGs, however, exhibit stable periodic orbits whose timing can be modified by inputs, meaning that sensory information never causes stepping to cease.

Much of the development and testing was conducted in the open-source simulation environment Animatlab, which consists of two primary segments: a neural dynamics simulator and a mechanical dynamics simulator.

The software allows the user to design a network of neurons to control muscles placed on a simulated animal model. *In vivo*, neurons express a wide range of capacitances, conductances, potential thresholds, and firing modes. The user can set all of these parameters and connect neurons by drawing synapses between cells. Just as with neurons, the type and properties of synapses can be set by the user based upon animal experimentation.

The neurons are modeled as single compartment leaky neurons with optional ion channel dynamics similar to those in the Hodgkin-Huxley model. Detailed spiking dynamics are not modeled, instead letting the membrane voltage of a neuron represent either one nonspiking neuron, a population of nonspiking neurons, or the spiking rate of a population of spiking neurons.

The change in a neuron's membrane potential, V_i is described by the following differential equation:

$$C_m \frac{dV_i}{dt} = -I_L(V_i) - \sum_{j \neq i} I_{syn}(V_j, V_i) + I_{app}$$

where C_m is the membrane capacitance of the neuron's membrane, $I_L(V_i) = g_L(V_i - E_L)$ is the leak current, I_{app} is the sum of all intrinsically or externally applied currents, and $I_{syn}(V_j, V_i) = g_{syn}s_\infty(V_j)(V_i - E_{syn,j})$ is the synaptic current from neuron j to neuron i . $s_\infty(V_j)$ is a sigmoid function that increases monotonically from 0 to 1 over the conductance range of the synapse, V_l to V_h ,

$$s_\infty(V_j) = \begin{cases} 0, & V_j < V_l \\ (V_j - V_l)/(V_h - V_l), & V_l \leq V_j \leq V_h \\ 1, & V_j > V_h \end{cases}$$

CPG units are made up of two pairs of neurons, each forming one half of a half-center oscillator. Each half-center pair consists of a neuron following equation 1 that is excited by a neuron with an additional term

$$C_m \frac{dV_i}{dt} = -g_{Ca}m_i h_i (V_i - E_{Ca}) - I_L(V_i) - \sum_{j \neq i} I_i(V_i, V_j) + I_{app}$$

where $I_{Ca}(V_i, m_i, h_i) = g_{Ca}m_i h_i (V_i - E_{Ca})$ is an additional nonlinear current term that models the influx of Ca^{2+} ions through voltage gated ion channels. The conductance of these ion channels is modulated by the fast opening and slow closing of gating variables m and h whose dynamics are described by

$$\frac{dm_i}{dt} = \frac{m_\infty(V_i) - m_i}{\tau_m(V_i)} \quad \frac{dh_i}{dt} = \frac{h_\infty(V_i) - h_i}{\tau_h(V_i)}$$

where $m_\infty(V_i)$ and $h_\infty(V_i)$ are, respectively, increasing and decreasing sigmoid functions in the range $[0, 1]$ and $\tau_m(V_i)$ and $\tau_h(V_i)$ determine the time scale at which m_i and h_i change. Additionally, for this group of neurons I_{app} provides enough tonic current to naturally depolarize the neuron. The oscillator is completed by inhibiting each calcium dependent neuron by the interneuron from the opposing half-center, forming the CPG unit seen in figure 19. The time course and phase plane plot in figure 19 illustrates how the CPG exhibits endogenous oscillations even in the absence of sensory input through a shift in the V-nullcline.

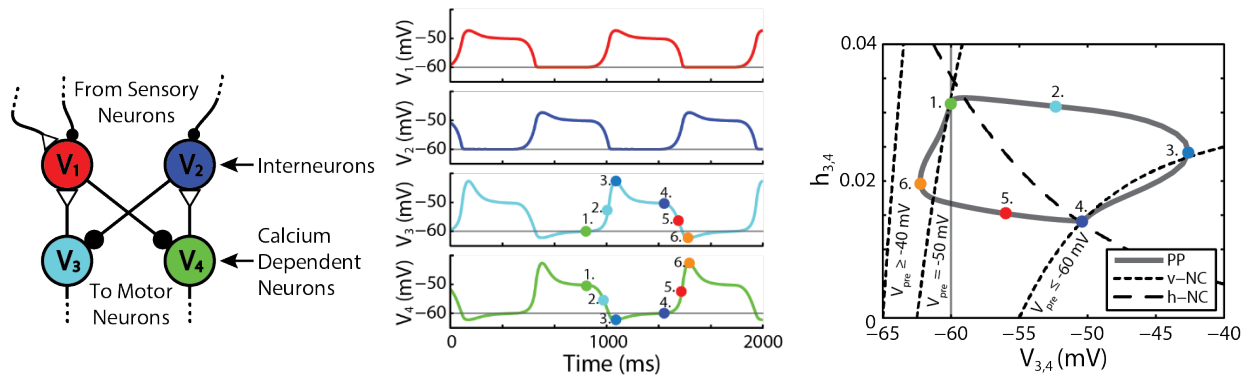


Figure 19: Small networks of neurons can exhibit endogenous oscillations. The timing of oscillation is influenced by the parameters of the neurons and synapses and can be altered through descending signals.

In addition to the neural editor, Animatlab includes a 3D modeling and dynamical simulator. The model is linked together through a series of joints, both ball-and-socket and hinge types. The bodies' kinematic and inertia properties can be set to match biological systems. In addition, meshes (a standard animation/video game 3D representation) can be imported, allowing the user to produce accurate models

of the physical world. Bodies' movements are simulated through the Vortex physics engine, a well-known and commonly used simulator.

Neural and mechanical systems can interact through a series of actuators and sensors. Muscles can be placed across joints, attached to bodies, and activated by the voltage level of a neuron. The muscles in Animatlab are based on the linear Hill muscle model, which treats muscles as a series of springs, dampers, and contractile units. The tension a muscle can apply is dependent on both the reactive properties of the mechanical approximation and the stimulus applied to the muscle. Stretch receptors, joint angle sensors, and force detectors are available to interface the simulated physical environment with the neural controllers.

Using these tools, our previous work, and available literature, a BNN LegConNet was designed for a middle cockroach leg. It generates coordinated, periodic motion by coupling central pattern generators (CPGs) via sensory information. The sensors used in the simulation are very similar to those in the animal and in the new robotic leg, so this transformation was relatively straightforward. For the robotic leg, additional functionality was added to interface between the neural circuitry and the servos, mimicking muscle dynamics.

Based upon animal neural organization, BNN LegConNet consists of four basic levels: sensory, integration, CPG, and motor. The implementation of these structures is shown in Fig. 20. We discovered that when the sensory level fed directly into the motor level, the oscillation was often halted due to stimulation by many different sources at different times. This model was composed of two levels of neurons in the most direct transformation from the finite state version of LegConNet. Afterward, in order to increase biological accuracy and improve stability, CPGs were implemented. A CPG's oscillatory output can be altered by applying stimulus current to one or both of the half-centers. However, signals that are too large in magnitude or frequency cause the system to become unstable. To counter this, sensory information from various sources is combined and then sent to the CPGs via an integrator level. These interneurons add various sensory influences and smooth the total signal, therefore increasing the stability of the entire system. Such an organization is known to exist in invertebrates, and is crucial for obtaining complex, coordinated leg movements.

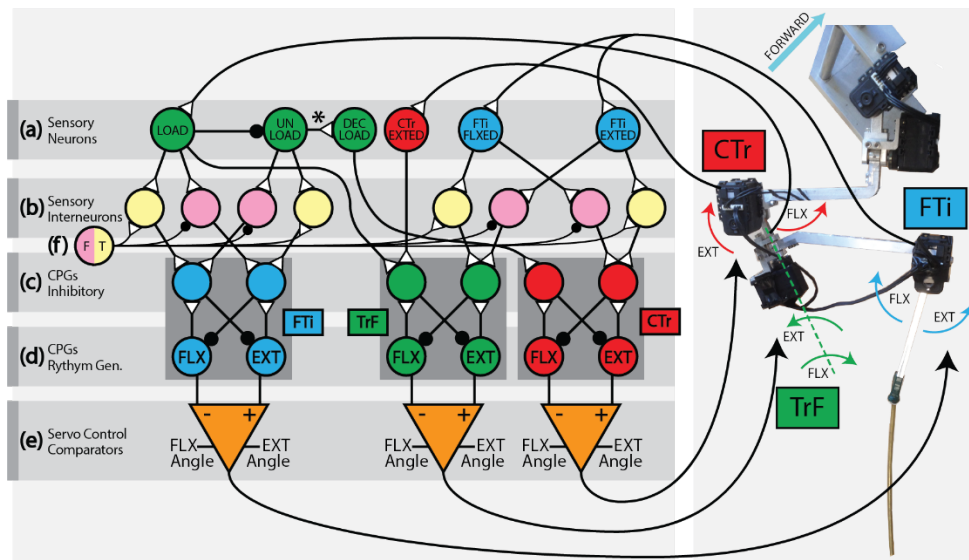


Figure 20: A visual representation of the biological neural network (BNN) used to control the model leg. Note the hierarchical structure of the network, and the way multiple CPGs are coordinated through sensory coupling from similar or the same sensory influences. Also note that only three joints are controlled by this network, since the movement of the two most proximal joints on the middle cockroach leg is very limited.

Once a basic circuit was designed and tested in Animatlab, a similar neural simulator testing environment was developed in LabVIEW so that the neural simulator could be interfaced with a NI CompactRIO-9074, which read from the physical sensors and controlled the Dynamixel AX-12+ smart servos on the robot. This also allowed for easy integration with the previously mentioned GUI interface and data acquisition and review software. Here, the neural dynamics are numerically integrated using an Euler one-step integration at 1000 Hz.

Sensory signals consist of joint angle and strain on the trochanter segment. Joint angles are read from the smart servos using a serial communication at 1 Mbps. Strain is measured using the previously mentioned strain gauges which are connected to a Wheatstone bridge, amplified and measured with a 16-bit ADC.

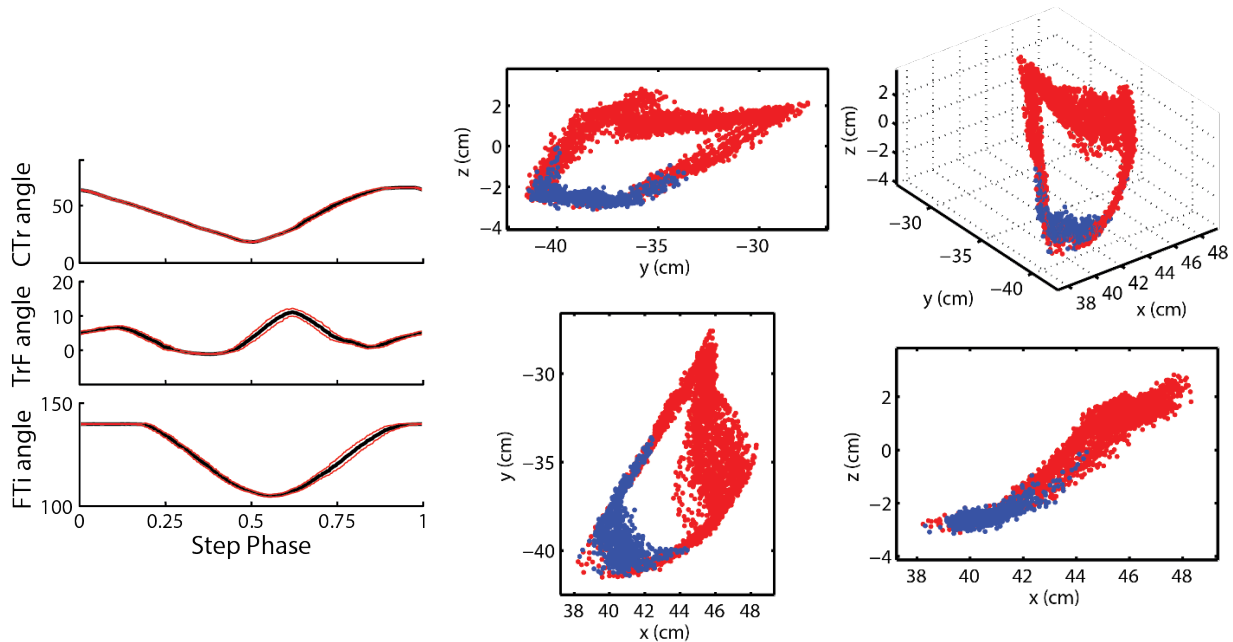


Figure 21: Typical joint angles and 3D tarsus positions during forward walking. Motions are very reproducible in the absence of external stimulation. $n=30$ steps. Red lines are an envelope of one standard deviation (left). The tarsus is on the ground when purple and raised when red (right).

The neural controller shown in figure 20 coordinates the three most distal joints, (Fti, TrF, and CTr), resulting in the stepping seen in Figure 21. Joint angles (left) as well as tarsus position (right) are reproduced reliably in the absence of external perturbations.

The model can exhibit different behaviors by altering the path of neural information from sensory neurons to the CPGs. This can be done by utilizing a gating neuron (f in figure 11) to suppress or excite sensory interneurons. In this way, interneurons are used like gates that can be opened or closed based on descending control of the gating neuron. Figure 22 illustrates a switch from forward walking to inside turning by switching paths of minimal neural signals. Tarsus position, as seen from above makes a qualitative shift from rotating straight rearward to pulling inside.

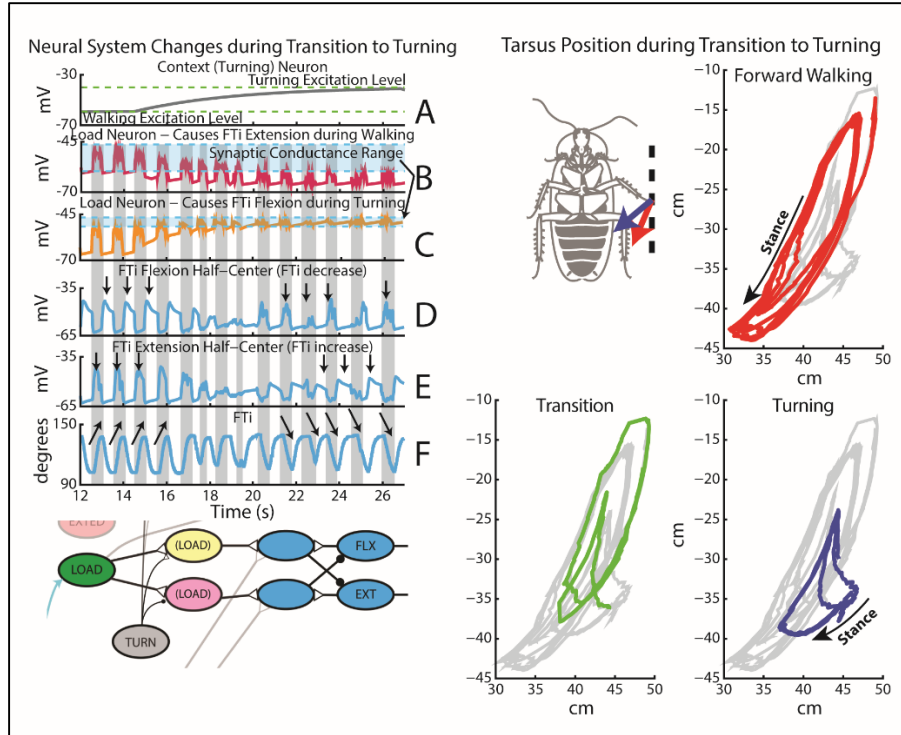


Figure 22: As the gating/context neuron becomes excited from a descending command, the red and yellow interneurons switch rolls, diverting the sensory signals to different sides of the CPG. This results in a phase shift of activity.

CPGs smooth and stabilize the sensory driven network: Because CPGs can oscillate with stable orbits without periodic inputs, a walking network driven by CPGs is inherently smoother and more stable than a purely sensory driven one. To test this, we made two versions of our middle leg controller: one with CPGs coupled by sensory feedback, and one in which the dynamics that cause endogenous oscillation were removed. This made the second model operate like the finite state machine version of LegConNet, in which

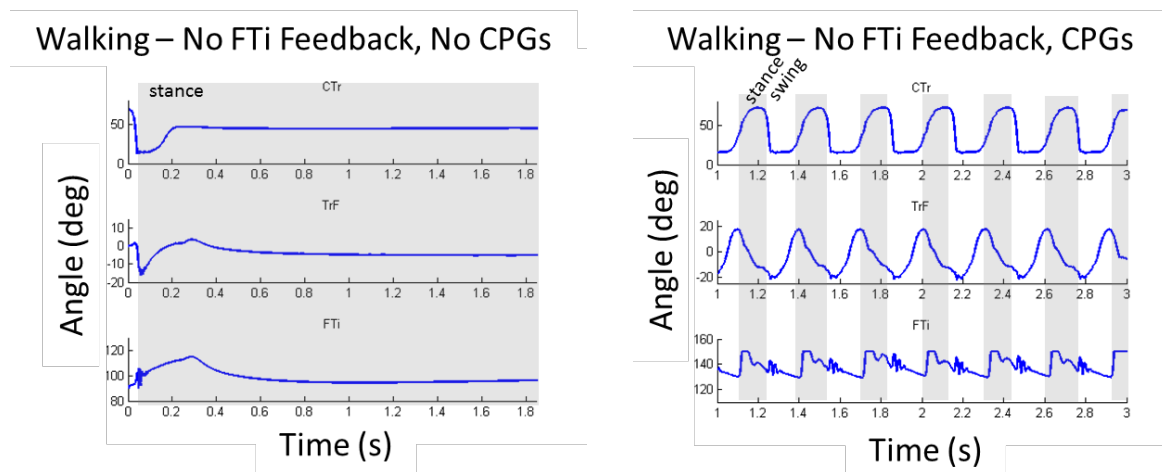


Figure 23: Comparison between trials in which the middle leg model was made to walk without CPGs (left) and with CPGs (right) after the connections to the FTi were removed. If any sensory information is missing the reflex chain stops; but CPGs maintain rhythmicity, even if some sensory information is missing. The shaded areas are when the leg is in stance phase.

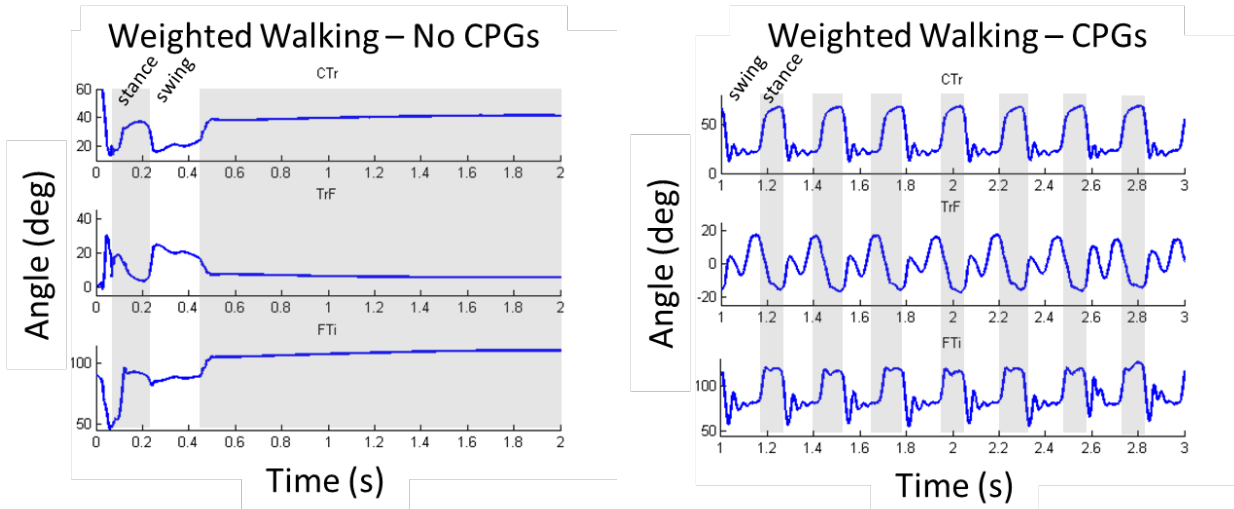


Figure 24: – Comparison between trials in which the middle leg model was made to walk without CPGs (left) and with CPGs (right) after the tibia’s weight was drastically increased. The extra load causes the leg without CPGs to take a single step and then remain in stance because the load signal overwhelms the reflex chain. However, the leg with CPGs is able to continue stepping, albeit with modified kinematics. The shaded areas are when the leg is in stance.

walking motions were generated by a reflex chain. Two experiments were then run to compare performance: ablating sensory pathways to one CPG, and loading the leg with additional weight.

Extreme situations may lead to loss of segments or legs, requiring insects to continue locomotion without expected sensory information. In addition, different terrains or environmental conditions may lead to locomotion in which the required sensory information is never obtained. Therefore, we tested our CPG model versus the no-CPG model and removed the connection to the FTi CPG (from load sensors). In the model without CPGs, this lack of sensory information broke the reflex chain, and walking halted. However, the model with CPGs could still function, even with limited sensory information. Kinematics from a trial are shown in figure 24.

Another experiment showed that CPGs make stepping more robust to changes in walking resistance, such as walking through a viscous material. In this test, the mass of the tibia was increased by a factor of ten. The leg was then made to walk. Again, the leg without CPGs could not continue to walk because the extra weight generated a large load signal, which overwhelmed the reflex chain. Kinematics from an example trial are shown in figure 24.

These experiments highlight the importance of endogenously oscillating CPGs to our model. Sensory feedback is important to coordinate and adapt locomotion to the environment, but is not sufficient to produce the robustness seen in animals. This work is an improvement over our finite state machine model in that it is more biologically accurate, analytically tractable, and robust to disturbances.

Examine Local Control of Moth Flight:

Background: The focus of the flight component of this project has been to observe and measure the effects of the tegula, a local feed back sensor thought to report on wing position and movement, on flight and flight control in the moth *Manduca sexta*. Until this project most of what is known about the tegulae and their role in flight has been learned from the locust, a more primitive and much less maneuverable flier than our moth.

Summary of Behavioral Deficits from Tegulae Lesions: We have now completed the behavioral studies demonstrating that surgical removal of the tegulae causes significant losses in the flight capabilities of the

moth *M. sexta*. Flying locusts have also been observed to loose aspects of their flight performance, but in a different way. The front and hind wings of locust are separate, have different shapes and beat slightly out of phase with each other, while our moths front and hind wings are mechanically linked and appear to beat as a single unit. So these two flying insects appear to use their wings differently during flight and we now know removal of the tegulae effects them differently. The larger hind wing of the locust develops most of the forces for flight, and the removal of the hind wing tegulae cause a significant drop in wing beat frequency, and a restriction in the ability to increase their altitude in flight. Loss of the tegulae from the front wing of locusts has no significant effect on their flight performance.

We removed all combinations of tegulae (i.e., one, two, three or four, front, hind, left, right, symmetrically, asymmetrically, etc.) from otherwise intact moths and compared their free flight performance in different experimental environments in our laboratory wind tunnel. We assessed the moths abilities to compensate for increased loads by challenging them to fly in different wind speeds (i.e., still air and 1 m/s). The ability perform specific tasks while flying was assessed by comparing flight in clean air to tracking a pheromone plume upwind. In all cases, it was only when all four tegulae had been removed that statistically significant effects on the performance were measured (Willis and Avondet, submitted).

Previously we reported that our hypothesis, that task-dependent descending input from the brain could improve the performance of teguale lesioned moths, has been supported by our experimental results. We have now tested this idea in two different ways by comparing lesioned and intact moths as they, fly in clean air vs. a wind-borne pheromone plume, and as they track a pheromone plume through an environment that provides normal visual feedback and one that provides nearly zero feedback of self motion. Recent analyses show that moths that have no tegulae take longer to warm up their flight muscles prior to taking flight, and that this effect is greater in the absence of visual feedback of their movements. Once these individuals take flight they fly for shorter durations when in the environment that provides little or no visual feedback from their flight movements (Fig. 25). The tegulae lesioned moths performed significantly worse than the intact moths, but those in enviroments that provided visual feedback of their movements performed better than those with little or no visual feedback.

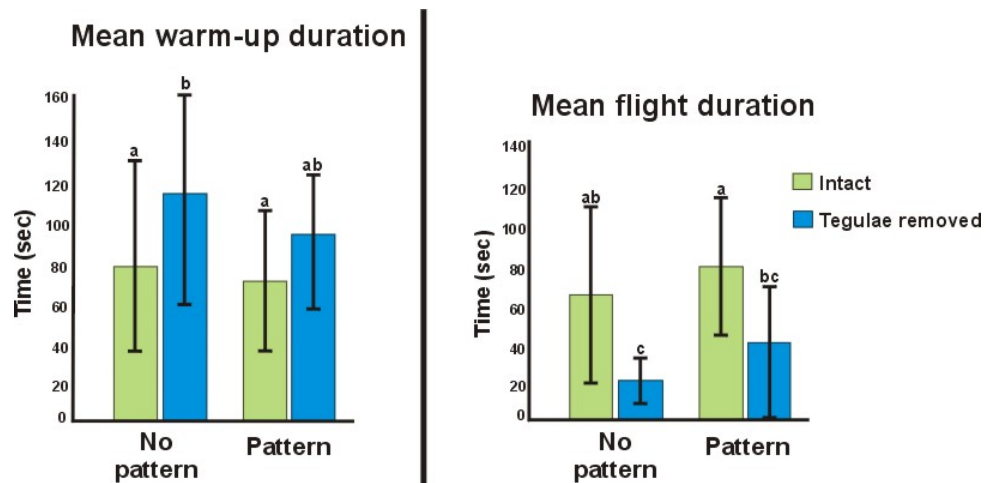


Figure 25: Mean (\pm S.D.) durations of pre-flight warm-up and free flight bouts of male moths with all tegulae removed and intact controls as they flew in environments that provided visual feedback (Pattern) of their movements and one that did not (No Pattern). Bars with no lowercase letters in common are significantly different according to a one-way ANOVA, $p < 0.05$.

Since tracking an odor plume in flight requires visual feedback, we also challenged our tegulae lesioned individuals to track pheromone plumes through the same high and near zero visual feedback environments described above. As before, fewer of the moths with no tegulae were able to successfully track a plume compared to the intact moths (Fig. 26). However, when a the moths flew above a floor pattern

of randomised dots (i.e. Pattern) it provided visual feedback of their flight movements and the moths that had lost all their tegulae increased their plume tracking successes by approximately 10 percent relative to the moths in the environment with out the visible pattern (Fig. 26). This further supports our idea that task-dependent descending information can “rescue” some moths that have lost all proprioceptive input from their tegulae. It also emphasizes the importance of visual feedback of self-motion for flight control.

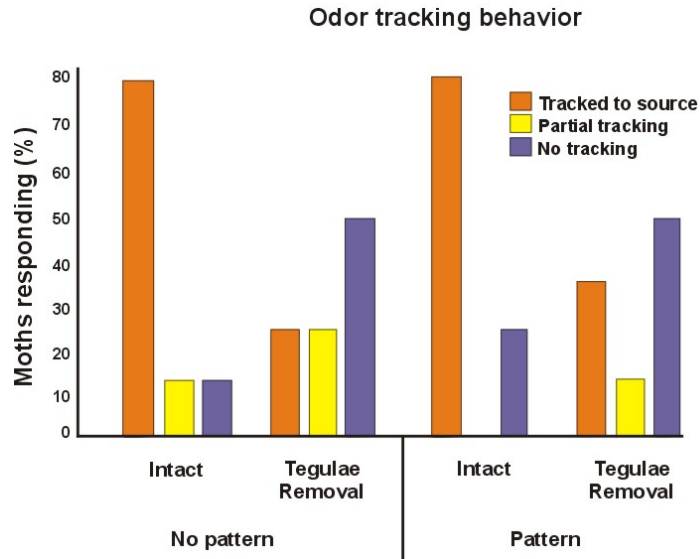


Figure 26: Proportion of intact and tegulae lesioned moths that were able to track a plume of sex attractant pheromone upwind to the source through environments that provided visual feedback of flight movements (Pattern), and those that provided no visual feedback (No pattern).

Brain Lesions Affect Plume Tracking Flight and May Cause Non-adaptive Turning: In the past year we have begun to conduct studies of the brain’s role in generating the descending inputs necessary to influence how the moths are able to respond to olfactory and visual inputs and recover some of the capabilities they lost when we removed their tegulae. We have begun to compare the plume tracking flight performances of moths before and after the introduction of focal brain lesions. We are using the studies of Harley and Ritzmann (2010) as a model. Our initial behavioral analysis shows that it may be difficult to identify lesion-induced deficits to flight control unless we challenge the moths to perform specific tasks. The ability activate in response to introduction to the pheromone plume and taking flight shows almost no impact of either the insertion of a lesioning electrode into the brain, or application of electrical current through that electrode (Fig. 27).

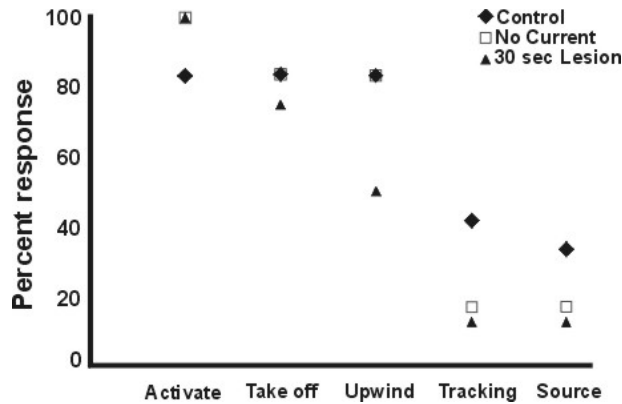
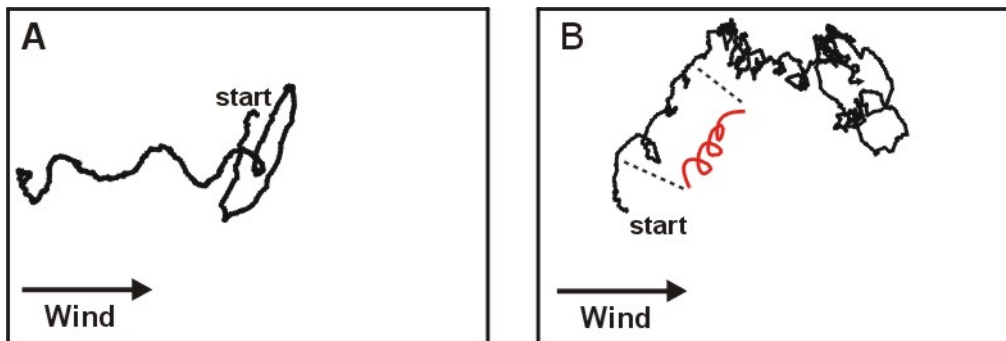


Figure 27: Percent of our experimental population of control and brain-lesioned moths responding to wind-borne pheromone plume with specific behavioral categories (n=15).

However, beginning with turning and orienting into the wind through source location, moths experiencing brain lesions perform worse than intact controls (Fig. 27). This is our initial stage of analysis of these results and studies identifying the placement of the lesion in the brains of these moths is ongoing. The detailed examination and measurements of the flight trajectories of these moths is also ongoing. We have included a sample of pre- and post-lesion flight tracks from one individual that showed a particularly interesting response to its brain lesion (Fig. 28). These tracks show a typical upwind plume tracking performance from the moth before its brain was lesioned (Fig. 28A). When the same animal was challenged to respond to a pheromone plume next day, after it had experienced a lesion in its central brain, it activated in response to pheromone, and took flight. However, as soon as it was flying it began to execute rightward turns until it landed. We do not yet know where in the brain this animal's lesion resides, but this continuous turning behavior has some similarities with turning behavior observed from cockroaches with lesions in the central complex (Harley and Ritzmann, 2010).



*Figure 28: Illustration of pre- (A) and post-lesion (B) flight tracks of a male *Manduca sexta* moth responding to wind-borne female sex-attractant pheromone. The red inset to panel B is a simplified and expanded view of the section of the track delineated by the dashed lines. The entire flight track is made up of a sequence of rightward looping turns executed just a few centimeters above the floor.*

Loss of Tegula Input and Free Flight Maneuvering: It is clear from our behavioral analyses that the loss of feedback from the tegulae during flight has significant effects on the flight trajectories of moths flying with no tegulae. We have now collected and begun to analyze a set of high speed video recordings of intact and complete tegulae lesioned moths (i.e., all four tegulae removed) tracking pheromone plumes in free flight, to determine how loss of tegulae input effects the movement of the wings that result in the loss of flight performance. It is our ultimate goal to collect recordings of flight muscle activation patterns simultaneously with high speed video recordings to associate specific changes in the flight motor patterns

with their effects on wing movements in tegulae lesioned moths. The movement of the wings during flight is caused by the activity of many flight muscles, and the current analysis is the first step toward identifying which muscles are likely to have altered activation patterns, and therefore should be targeted for free flight motor recordings. This step is necessary because, although *M. sexta* is a large robust insect that will carry electrodes in their muscles during free flight, minimizing the number of electrodes ensures we will be studying the effects of tegulae removal and not the added load of the electrodes.

A sub-sample from our ongoing analysis suggests that the wing beat frequency is one element of the flight motor that is not effected by tegulae removal in freely flying moths. We have measured the duration of five wing beat cycles from three different intact control moths and three moths with all four tegulae removed and discovered that their mean wing beat frequencies are essentially identical (Intact control = $10.6 \pm 0.92\text{Hz}$; Complete tegulae removal = $10.5 \pm 0.12\text{Hz}$). These data are at odds with our measurements of tethered flying moths which show that after removal of all the tegula the wing beat frequency of most moths decreases. These recent measurements from freely flying moths suggest that providing all of the sensory information associated with actually flying may allow the nervous systems of these tegulae-lesioned moths to maintain their wing beat frequencies in the normal range relative to intact controls. Our ongoing experiments will begin to reveal how loss of tegulae inputs effects the flight of these moths and how their nervous systems adapt to this loss to maintain some flight capabilities.

Activity of mechanosensors on the tegulae: Since our previous reports we have made initial neurophysiological recordings from the sensory nerve innervating the tegulae (Fig. 29). We are still developing the final version of the preparation to characterize the activation of the tegula during the wing beat cycle. This preparation will almost certainly require that the recordings be made from tethered flying moths (i.e. intact moths free to flap their wings while held attached to a metal rod). It has been a significant challenge to develop a simple practical way of recording from this small nerve when the moth is restrained. The nerve branch connecting the tegulae to the CNS is part of a larger nerve that carries all of the sensors on the wing. Great care must be taken to maintain connectivity between the wings and the flight circuitry in the thoracic ganglia because without this it is nearly impossible to stimulate flight. Because of this it may be extremely difficult to transition these recordings to freely flying moths, which has always been the ultimate goal. We have conducted pilot studies aimed at using high speed video cameras to characterize the physical relationships between the movements of the wings and the tegulae in tethered flying moths. These techniques will be combined and synchronized with the electrophysiological recordings of the tegula nerve using the same methods used to synchronize our flight muscle recordings and the high speed video of freely flying moths in the wind tunnel (please see below).

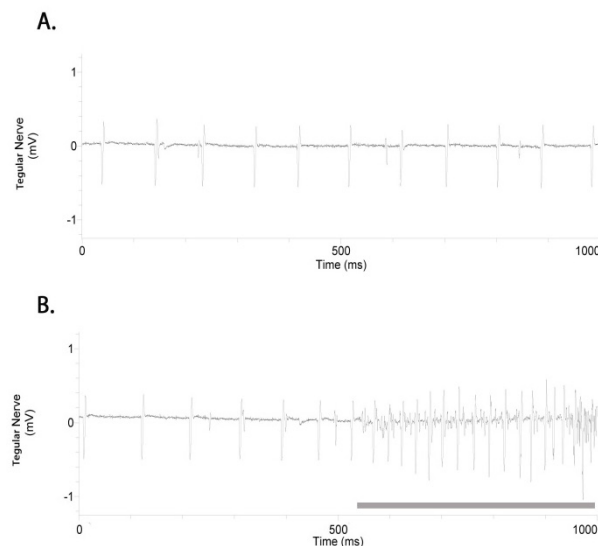


Figure 29: Hook electrode recordings from right forewing tegular nerve A. Baseline neural activity, B. Changes in activity upon stimulation by gently touching mechanosensory hairs (gray bar).

Effect of loss of tegula input on flight muscle activity and wing movements: Excellent progress was made in determining the effects of the loss of sensory input about wing movement on the control of flapping flight in the moth *Manduca sexta*. Building on our earlier behavioral studies demonstrating that loss of input from the tegulae has significant effects on moth flight trajectories, we have now begun to understand how loss of tegulae inputs alters the activation patterns of the major muscle groups causing wing flapping. By taking advantage of the large size and impressive flight capabilities of *M. sexta* we are using high speed video and fine-wire electrodes to compare flight muscle activation patterns and their associated wing and body movements between freely flying moths with and without their tegulae. For our first experiment we have focused on the activity of the muscles whose contraction generates the most obvious movements of flight, the upstroke and downstroke of the wings. We have focused on these muscles because they are large and easy to record from, and because we can compare our results to what is known about motor patterns and tegulae loss from freely flying locusts (Kutsch et al., 2003). So far these data confirm our previous behavioral studies showing that loss of tegulae input has variable effects, with some individuals unable to take flight and the performance of others indistinguishable from normal moths. So far these data confirm our earlier behavioral studies showing that loss of tegulae input renders some individuals unable to fly while the flight of others is indistinguishable from intact normal moths. In many cases, differences between the moths with and without their tegulae can be subtle. The moths with no tegulae, that can fly, generate almost the same wing beat frequency as intact moths (Table 1). A constant wing beat frequency in different environmental conditions is consistent with earlier studies of intact moths (Willis et al., 2000; Willmott and Ellington, 1997).

*Table 1: Means (\pm S.D.) of the instantaneous firing frequency of the main wing depressor and elevator muscles and phase of activation of elevator muscles with respect to depressor activity of *M. sexta* males tracking odor plumes upwind.*

<i>Treatment</i>	<i>Instantaneous Frequency</i>				<i>Phase</i>
	<i>L depressor</i> (Hz)	<i>R depressor</i> (Hz)	<i>L elevator</i> (Hz)	<i>R elevator</i> (Hz)	<i>Elevators</i> (degrees)
<i>Tegulae Intact</i>	25.3 \pm 1.3	24.2 \pm 0	24.9 \pm 1.3	25.3 \pm 1.4	183.6 \pm 19.7
<i>Tegulae Removed</i>	24.7 \pm 2.1	24.9 \pm 1.7	25.0 \pm 1.6	24.8 \pm 1.4	145.2 \pm 24.0

However, in the locust, the only other insect in which this has been studied, loss of tegulae input causes a decrease in wing beat frequency (Fischer and Ebert, 1999; Kutsch et al., 2003). Other variables characterizing the flight muscle activation patterns, such as the duration of muscle activation are also similar. However, the timing of activation of the upstroke muscles with respect to the downstroke muscles, or their phase of activation, is significantly different. Moths flying without tegulae input activate their elevator muscles much sooner in each wing beat cycle than the normal moths (Table 1). It is possible that this early upstroke activation could shorten the normal downstroke which could result in less lift generated with each wing beat. One of the most consistent characteristics of flight with no tegulae input, in locusts and moths, is an inability to gain altitude. This change in the relative timing of muscle activation could account for at least part of this loss of normal performance. We are still in the process of measuring

the wing and body movements associated with the flight motor patterns, but what we have measured supports the idea that the altered timing of elevator muscle activation may partially explain the loss in flight performance. Our data shows that moths which had their tegulae surgically removed generate smaller wing stroke amplitudes than the intact control moths (Table 2), as one might predict based on their shifted elevator activity.

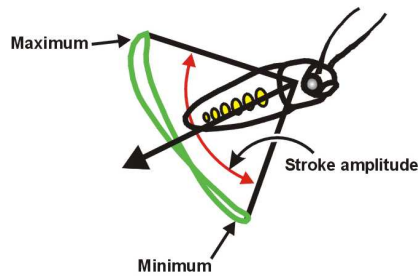


*Table 2. Mean (+S.D.) wing stroke amplitudes of *M. sexta* males with and without their tegulae flying upwind in an odor plume.*

<i>Treatment</i>	<i>n</i>	<i>Stroke Amplitude (degrees)</i>	
		<i>Left Wing</i>	<i>Right Wing</i>
<i>Tegula Intact</i>	3	85.2 ± 6.0	90.9 ± 19.9
<i>Tegula Removed</i>	3	79.9 ± 7.4	81.6 ± 9.4

Thus far our results show that the moth flight control system may be using the information provided by the tegulae differently than the much better understood locust flight system (Fischer and Ebert, 1999; Fischer et al., 2002). Unlike *M. sexta*, freely flying locusts have significantly lower wing beat frequencies after their tegulae are removed and there is no effect on the relative timing of activation of their elevator muscles (Fischer and Ebert, 1999). Although there are many variables associated with the muscle activation and wing movements underlying flight behavior, it is interesting that even with their obvious differences, the overall effect of the loss of tegulae input on locusts and moths is similar – a loss of ability to climb, or increase their altitude. We have good reason to study the effect of tegulae loss on the wing elevator muscles, because of the well-known direct connections between the tegulae sensory cells and the elevator motor neurons in the locust flight system. However, it is possible that the ability of moths (and perhaps locusts) to continue to fly and maneuver after the loss of tegulae input may be caused by the same type of descending input from the brain demonstrated by the Ritzmann lab group to affect the walking control system in the cockroach. For this reason, upon completion of our analysis of the effect of tegulae loss on the wing elevator and depressor muscles we will characterize changes in selected steering muscles associated with the loss of the tegulae. These so-called steering muscles can alter the production of lift and thrust by changing the details of the position and movement of the wings during each wing beat. Changing their activation, and thus the structure of the wing stroke, could compensate in part for the abnormal activation of the wing elevators associated with tegulae loss.

Summary

This report documents our accomplishments over the 4 years that we were funded by AFOSR grant. We have accomplished all of the goals set out in the initial proposal. The data that was collected clearly supports our initial hypothesis that changes in direction of movement is accomplished through brain centers examining exteroceptors in the context of physiological state then generating appropriate descending commands that alter critical local reflexes. While this model is supported both by biological data on walking and flying insects and by our modeling efforts, the situation revealed by our arena studies is far more complex. This is to be expected in the less controlled and closed loop conditions of freely walking and foraging insects. By examining these hypotheses in a range of experimental situations (restrained, tethered and freely moving in complex environments) we believe that our data has led to fundamental neuroethological principles of animal navigation that will make them invaluable to numerous Department of Defense projects. We further believe that the praying mantis now presents an opportunity to take these findings to even greater and more important levels.

References

- Akay, T., Haehn, S., Schmitz, J. and Büschges, A. (2004). Signals from load sensors underlie interjoint coordination during stepping movements of the stick insect leg. *J Neurophysiol* 92, 42-51.
- Akay, T., Ludwar, B. C., Goritz, M. L., Schmitz, J. and Büschges, A. (2007). Segment Specificity of Load Signal Processing Depends on Walking Direction in the Stick Insect Leg Muscle Control System. *J. Neurosci.* 27, 3285-3294.
- Bender, J. A., Pollack, A. J. and Ritzmann, R. E. (2010a). Neural Activity in the Central Complex of the Insect Brain Is Linked to Locomotor Changes. *Curr. Biol.* 20, 921-926.
- Bender, J. A., Simpson, E. M. and Ritzmann, R. E. (2010b). Computer-Assisted 3D Kinematic Analysis of All Leg Joints in Walking Insects. *PLoS One* 5, e13617.doi:10.1371/journal.pone.0013617.
- Bender, J. A., Simpson, E. M., Tietz, B. R., Daltorio, K. A., Quinn, R. D. and Ritzmann, R. E. (2011). Kinematic and behavioral evidence for a distinction between trotting and ambling gaits in the cockroach *Blaberus discoidalis*. *J. Exp. Biol.* 214, 2057-2064.
- Borgmann, A., Hooper, S. L. and Büschges, A. (2009). Sensory feedback induced by front-leg stepping entrains the activity of central pattern generators in caudal segments of the stick insect walking system. *J Neurosci* 29, 2972-83.
- Borgmann, A., Scharstein, H. and Büschges, A. (2007). Intersegmental coordination: influence of a single walking leg on the neighboring segments in the stick insect walking system. *J Neurophysiol* 98, 1685-96.
- Brown, A. E. (2011). Multi-legged Joint Kinematic Analysis of an Insect Tethered Over a Slippery Surface. In *Biology*, vol. MS, pp. 87. Cleveland, OH: Case Western Reserve University.
- Büschges, A. (1995). Role of local nonspiking interneurons in the generation of rhythmic motor activity in the stick insect. *J. Neurobiol.* 27, 488-512.
- Büschges, A. and Gruhn, M. (2008). Mechanosensory feedback in walking: from joint control to locomotory patterns. *Adv. Insect Physiol.* 34, 194-234.
- Büschges, A., Schmitz, J. and Bässler, U. (1995). Rhythmic patterns in the thoracic nerve cord of the stick insect induced by pilocarpine. *J. Exp. Biol.* 198, 435-456.
- Camhi, J. M. and Johnson, E. N. (1999). High-frequency steering maneuvers mediated by tactile cues: antennal wall-following in the cockroach. *J. Exp. Biol.* 202, 631-43.
- Canonge, S., Sempo, G., Jeanson, R., Detrain, C. and Deneubourg, J. L. (2009). Self-amplification as a source of interindividual variability: Shelter selection in cockroaches. *J. Insect Physiol.* 55, 976-982.
- Cowan, N. J., Lee, J. and Full, R. J. (2006). Task-level control of rapid wall following in the American cockroach. *J. Exp. Biol.* 209, 1617-1629.
- Daltorio, K. A., Tietz, B. R., Bender, J. A., Webster, V. A., Szczecinski, N. S., Branicky, M. S., Ritzmann, R. E. and Quinn, R. D. (2012). A Stochastic Algorithm for Explorative Goal Seeking Extracted from Cockroach Walking Data. In *IEEE ICRA*, pp. 2261-2268. St. Paul, MN.
- Daltorio, K. A., Tietz, B. R., Bender, J. A., Webster, V. A., Szczecinski, N. S., Branicky, M. S., Ritzmann, R. E. and Quinn, R. D. (2013). A model of exploration and goal-searching in the cockroach, *Blaberus discoidalis*. *Adapt. Behav.* 21, 404-420.
- Daun-Gruhn, S. and Büschges, A. (2011). From neuron to behavior: dynamic equation-based prediction of biological processes in motor control. *Biol. Cybern.* 105, 71-88.
- Ekeberg, Ö., Blümel, M. and Büschges, A. (2004). Dynamic simulation of insect walking. *Arth. Struct. Dev.* 33, 287-300.

- Fischer, H. and Ebert, E. (1999). Tegula function during free locust flight in relation to motor pattern, flight speed and aerodynamic output. *J. Exp. Biol.* 202, 711-721.
- Fischer, H., Wolf, H. and Büschges, A. (2002). The locust tegula: kinematic parameters and activity pattern during the wing stroke. *J. Exp. Biol.* 205, 1531-1545.
- Guo, P., Pollack, A. J., Varga, A. G., Martin, J. P. and Ritzmann, R. E. (2014). Extracellular Wire Tetrode Recording in Brain of Freely Walking Insects. *J. Vis. Expt.* 86, e51337.
- Guo, P. and Ritzmann, R. E. (2013). Neural activity in the central complex of the cockroach brain is linked to turning behaviors. *J. Exp. Biol.* 216, 992-1002.
- Halloy, J., Sempo, G., Caprari, G., Rivault, C., Asadpur, M., Tache, F., Said, I., Durier, V., Canonge, S., Ame, J. M. et al. (2007). Social integration of robots into groups of cockroaches to control self-organized choices. *Science* 318, 1155-1158.
- Harley, C. M., English, B. A. and Ritzmann, R. E. (2009). Characterization of obstacle negotiation behaviors in the cockroach, *Blaberus discoidalis*. *J. Exp. Biol.* 212, 1463-1476.
- Harley, C. M. and Ritzmann, R. E. (2010). Electrolytic lesions within central complex neuropils of the cockroach brain affect negotiation of barriers. *J. Exp. Biol.* 213, 2851-2864.
- Hellekes, K., Blincow, E., Hoffmann, J. and Büschges, A. (2012). Control of reflex reversal in stick insect walking: effects of intersegmental signals, changes in direction, and optomotor-induced turning. *J. Neurophysiol.* 107, 239-249.
- Homborg, U. (1987). Structure and functions of the central complex in insects. In *Arthropod brain: its evolution, development, structure and functions*, (ed. A. Gupta), pp. 347-367. New York: Wiley.
- Jindrich, D. L. and Full, R. J. (2002). Dynamic stabilization of rapid hexapedal locomotion. *J. Exp. Biol.* 205, 2803-2823.
- Kahsai, L., Martin, J.-R. and Winther, A. M. E. (2010). Neuropeptides in the Drosophila central complex in modulation of locomotor behavior. *J. Exp. Biol.* 213, 2256-2265.
- Kathman, N. D., Kesavan, M. and Ritzmann, R. E. (2014). Encoding wide-field motion and direction in the central complex of the cockroach *Blaberus discoidalis*. *J. Exp. Biol.* 217, 4079-4090.
- Klein, M. A., Brown, A. E., Li, W., Zill, S. N., Quinn, R. D. and Ritzmann, R. E. (2011). Biological observation and robotic modeling to understand leg control in the cockroach *Blaberus discoidalis*. *Soc. Neurosci. Abstr.* 37, 944.02.
- Koditschek, D. E., Full, R. J., Buehler, M. and (2004). Mechanical aspects of legged locomotion control. *Arth. Struct. Dev.* 33, 251-272.
- Kutsch, W., Berger, S. and Kautz, H. (2003). Turning manoeuvres in free-flying locusts: Two-channel radio-telemetric transmission of muscle activity. *J. comp. Zool. Part A* 299A, 139-150.
- Meyer, D. J., Margiotta, J. F. and Walcott, B. (1981). The shadow response of the cockroach, *Periplaneta americana*. *J. Neurobiol.* 12, 93-96.
- Mu, L. and Ritzmann, R. E. (2005). Kinematics and Motor Activity during Tethered Walking and Turning in the Cockroach, *Blaberus discoidalis*. *J. Comp. Physiol. A*. 191, 1037-1054.
- Mu, L. and Ritzmann, R. E. (2008a). Interaction between descending input and local thoracic reflexes for joint coordination in cockroach turning: I. Descending influence on thoracic sensory reflexes. *J. Comp. Physiol. A* 194, 293-298.

- Mu, L. and Ritzmann, R. E. (2008b). Interaction between descending input and local thoracic reflexes for joint coordination in cockroach turning: II. Comparative studies on tethered turning and searching. *J. Comp. Physiol. A* 194, 299-312.
- Nishiyama, K., Okada, J. and Toh, Y. (2007). Antennal and locomotor responses to attractive and aversive odors in the searching cockroach. *J. Comp. Physiol. A* 193, 963–971.
- Okada, J. and Toh, Y. (1998). Shade Response in the Escape Behavior of the Cockroach, *Periplaneta americana*. *Zool. Sci.* 15, 831-835.
- Okada, J. and Toh, Y. (2006). Active tactile sensing for localization of objects by the cockroach antenna. *J. Comp. Physiol. A* 192, 715–726.
- Orlovsky, G. N., Deliagina, T. G. and Grillner, S. (1999). *Neuronal Control of Locomotion: From Mollusc to Man*. Oxford, England: Oxford University Press.
- Ridgel, A. L., Alexander, B. E. and Ritzmann, R. E. (2007). Descending control of turning behavior in the cockroach, *Blaberus discoidalis*. *J. Comp. Physiol. A* 193, 385–402.
- Ritzmann, R. E. and Büschges, A. (2007). Adaptive motor behavior in insects. *Curr. Opin. Neurobiol.* 17, 629-636.
- Ritzmann, R. E. and Eaton, R. C. (1997). Neural substrates for initiation of startle responses. In *Neurons, Networks, And Motor Behavior*, eds. Paul S.G. Stein S. Grillner A. I. Selverston and D. G. Stuart), pp. 33-44. Cambridge, Massachusetts: MIT Press.
- Ritzmann, R. E., Harley, C. M., Daltorio, K. A., Tietz, B. R., Pollack, A. J., Bender, J. A., Guo, P., Horomanski, A. L., Kathman, N. D., Nieuwoudt, C. et al. (2012). Deciding Which Way to Go: How Do Insects alter Movements to Negotiate Barriers? *Front. Neurosci.* 6, doi: 10.3389/fnins.2012.00097.
- Ritzmann, R. E., Ridgel, A. L. and Pollack, A. J. (2008). Multi-unit recording of antennal mechanosensitive units in the central complex of the cockroach, *Blaberus discoidalis*. *J. Comp. Physiol. A* 194, 341-360.
- Rutter, B. L., Bender, J. A., Taylor, B. K., Ritzmann, R. E. and Quinn, R. D. (2008). Experiments in locomotion with neuromechanically based robotic insect models. *Soc. Neurosci. Abstr.* CD ROM 34, 198.7.
- Strausfeld, N. J. (1999). A brain region in insects that supervises walking. *Prog. Brain Res.* 123, 273-284.
- Szczecinski, N., Brown, A., Bender, J., Quinn, R. and Ritzmann, R. (2014). A neuromechanical simulation of insect walking and transition to turning of the cockroach *Blaberus discoidalis* *Biol. Cybern.* 108, 1-21.
- Tietz, B. R., Daltorio, K. A., Bender, J. A., Porr, D. A., J. T. Richards, J. T., Szczecinski, N. S., Webster, V. A., Quinn, R. D. and Ritzmann, R. E. (2011). Robotic modeling of goal directed behavior in the cockroach *Blaberus discoidalis*. *Soc. Neurosci. Abstr.* 37, 944.05.
- Watson, J. T., Ritzmann, R. E. and Pollack, A. J. (2002a). Control of obstacle climbing in the cockroach, *Blaberus discoidalis* II. Motor activities associated with joint movement. *J. Comp. Physiol. A* 188, 55-69.
- Watson, J. T., Ritzmann, R. E., Zill, S. N. and Pollack, A. J. (2002b). Control of obstacle climbing in the cockroach, *Blaberus discoidalis* I. Kinematics. *J. Comp. Physiol. A* 188, 39-53.
- Willis, M. A., Johnstone, L. and Costy-Bennett, S. J. (2000). Modulation of locomotory motor patterns in response to increased force requirements. *Soc. Neurosci. Abst Online.*, Program No. 643.3.
- Willmott, A. and Ellington, C. (1997). The mechanics of flight in the hawkmoth *Manduca sexta* 1. Kinematics of hovering and forward flight. *J. Exp. Biol.* 200, 2705-2722.
- Zill, S. N., Schmitz, J. and Büschges, A. (2004). Load sensing and control of posture and locomotion. *Arth. Struct. Dev.* 33, 273-286.